Journal of Electron Microscopy **61(6)**: 343–365 (2012)
doi: 10.1093/jmicro/dfs082

Biological: Review

Visualization of yeast cells by electron microscopy

Masako Osumi[1,2,*]

[1]Laboratory of Electron Microscopy/Bio-imaging Center, Japan Women's University, 2-8-1 Mejirodai, Bunkyo-ku, Tokyo 112-8681, Japan and [2]NPO: Integrated Imaging Research Support, 1-7-5-103, Hirakawa-cho, Chiyoda-ku, Tokyo 102-0093, Japan
*To whom correspondence should be addressed. E-mail: osumi@fc.jwu.ac.jp

Abstract In the 1970s, hydrocarbon or methanol utilizable yeasts were considered as a material for foods and ethanol production. During the course of studies into the physiology of yeasts, we found that these systems provide a suitable model for the biogenesis and ultrastructure research of microbodies (peroxisomes). Microbodies of hydrocarbon utilizing *Candida tropicalis* multiply profusely from the preexisting microbody. β oxidation enzymes in the microbody were determined by means of immunoelectron microscopy. We examined the ultrastructure of *Candida boidinii* microbodies grown on methanol, and found a composite crystalloid of two enzymes, alcohol oxidase and catalase, by analyzing using the optical diffraction and filtering technique and computer simulation. We established methods for preparing the protoplasts of *Schizosaccharomyces pombe* and conditions for the complete regeneration of the cell wall. The dynamic process of cell wall formation was clarified through our study of the protoplasts, using an improved ultra high resolution (UHR) FESEM S-900 and an S-900LV. It was found that β-1,3-glucan, β-1,6-glucan and α-1,3-glucan, as well as α-galactomannan, are ingredients of the cell wall. The process of septum formation during cell division was examined after cryo-fixation by high pressure freezing (HPF). It was also found that α-1,3- and β-1,3-glucans were located in the invaginating nascent septum, and later, highly branched β-1,6-glucan also appeared on the second septum. The micro-sampling method, using a focused ion beam (FIB), has been applied to our yeast cell wall research. A combination of FIB and scanning transmission electron microscopy is useful in constructing 3D images and analyzing the molecular architecture of cells, as well as for electron tomography of thick sections of biological specimens.

Keywords yeast, microbody (peroxisome), cell wall formation, *Schizosaccharomyces pombe*, ultra-low temperature/low-voltage scanning electron microscopy (ULT/LVSEM), FIB-STEM

Received 4 October 2012, accepted 9 November 2012; online 10 December 2012

Introduction

Yeasts are unicellular eukaryotes, and have fundamentally the same subcellular structure as higher animal and plant cells, and are used widely as a model system in basic and applied fields of life science, medicine and biotechnology. The National Institutes of Health, USA, designates yeasts as one of model organisms for biomedical research.

The ultrastructure of yeast cells was first studied by transmission electron microscopy (TEM) using thin sections in 1957 [1], and the freeze-etching replica method was introduced in 1969; at that

point the fine structure of yeast cells was obtained [2]. During the next 50 years, techniques for analyzing ultrastructure of yeasts advanced greatly. Here, I will review the development of fixation methods, rapid-freeze techniques and instruments for studying yeasts by use of electron microscopy (EM). Our discovery of fine structure and of enzymes of microbodies is shown, and the process and mechanism of septum formation as well as the ultrastructure, components and mechanism of formation of cell wall, will be described in this review. Finally, I will introduce a perspective on yeast ultrastructure research in the 21st century.

General features of yeast cells and the development of their fixing techniques

The yeast is classified into the budding yeast and the fission yeast. The budding yeast (Fig. 1a) has an ellipsoidal shape ($6 \times 5\,\mu m$), and divides by budding. On the other hand, fission yeast (Fig. 1c) has a cylindrical rod-shape ($7–8 \times 2.5\,\mu m$), and divides by medial fission. Although yeasts have these two types of cell proliferation, the cellular structures are basically the same as each other: nucleus with nuclear pores, mitochondria, microbodies, vacuoles, endoplasmic reticulum, and so on. Golgi apparatus is rarely observed as a 'fence' in budding yeast, but its stacks appear usually in fission yeast (Fig. 1b and d).

At the late 1950s, I began to develop the technique of fixation of yeast cells for the study by use of EM, because yeasts have a thick cell wall composed of an inner network of glucans and an outer layer of mannoproteins, which is a barrier to penetration of osmium tetroxide (OsO_4) solution, which is widely used as a fixative for many organisms. Figure 2 shows the progress of fixation methods and corresponding TEM images of yeasts from 1957 to 1985. Yeast cells were fixed solely with potassium permanganate ($KMnO_4$) and EM photographs were taken by me in the early 1960s (Fig. 2a and b) [3]. More fine EM images that were obtained by using double fixation with and $KMnO_4$ (Fig. 2c) made us able to study the ultrastructure in relation to cellular function [4]. To remove the yeast cell wall, we digested cells with Zymolyase (β-1,3-glucanase) [5], and obtained complete protoplasts. In the middle of the 1970s, our research team succeeded in obtaining a good EM image of the spheroplast or protoplast fixed with glutaraldehyde (GA) and OsO_4 (Fig. 2d) [6].

However, the information on the cell wall was lost using this method. Then, the rapid freezing of yeast cells using a sandwich method was achieved [7], and finally we were able to realize the whole cell image of yeast cells with natural cell wall (Fig. 2e). Thus, we could now easily analyze images of the same specimen by use of both TEM and scanning electron microscopy (SEM), and hence we started studies on morphology of the yeast cell by high resolution (HR) and low voltage (LV) SEM [8].

To get a large quantity of frozen yeast cells for diversified analyses, we developed the HPF method [9–14]. Then, freeze-etching method and microsampling methods, using focused ion beam [FIB, see FIB-scanning transmission electron microscopy (STEM) is useful for cell biology Section] as well as thin sectioning, can be applied for both budding and fission yeast cells, for observation with TEM and SEM, the same as other organisms. Figure 3 shows the progress of model image of yeast cell ultrastructure, and changes in fixation methods during the last 30 years [9]. $KMnO_4$ fixation is still useful for visualizing cell walls, in order to examine mating and germination processes [15].

Fine structure and biogenesis of microbodies (peroxisomes) in hydrocarbon utilizable yeast, *Candida tropicalis*, grown under different carbon sources

Fine structure of microbody

In the early stages of biotechnology, hydrocarbon or methanol utilizable yeasts were considered as a material for foods and ethanol production. Although the metabolism and fermentation of hydrocarbons producing useful substances have been extensively studied in this period, only few reports have been published about the relation between ultrastructure and metabolism [16,17]. During the course of studies of the physiology of hydrocarbon-utilizing yeasts, we found that microbodies that have a homogeneous matrix and are surrounded by single unit membranes appeared profusely in various strains of *Candida*

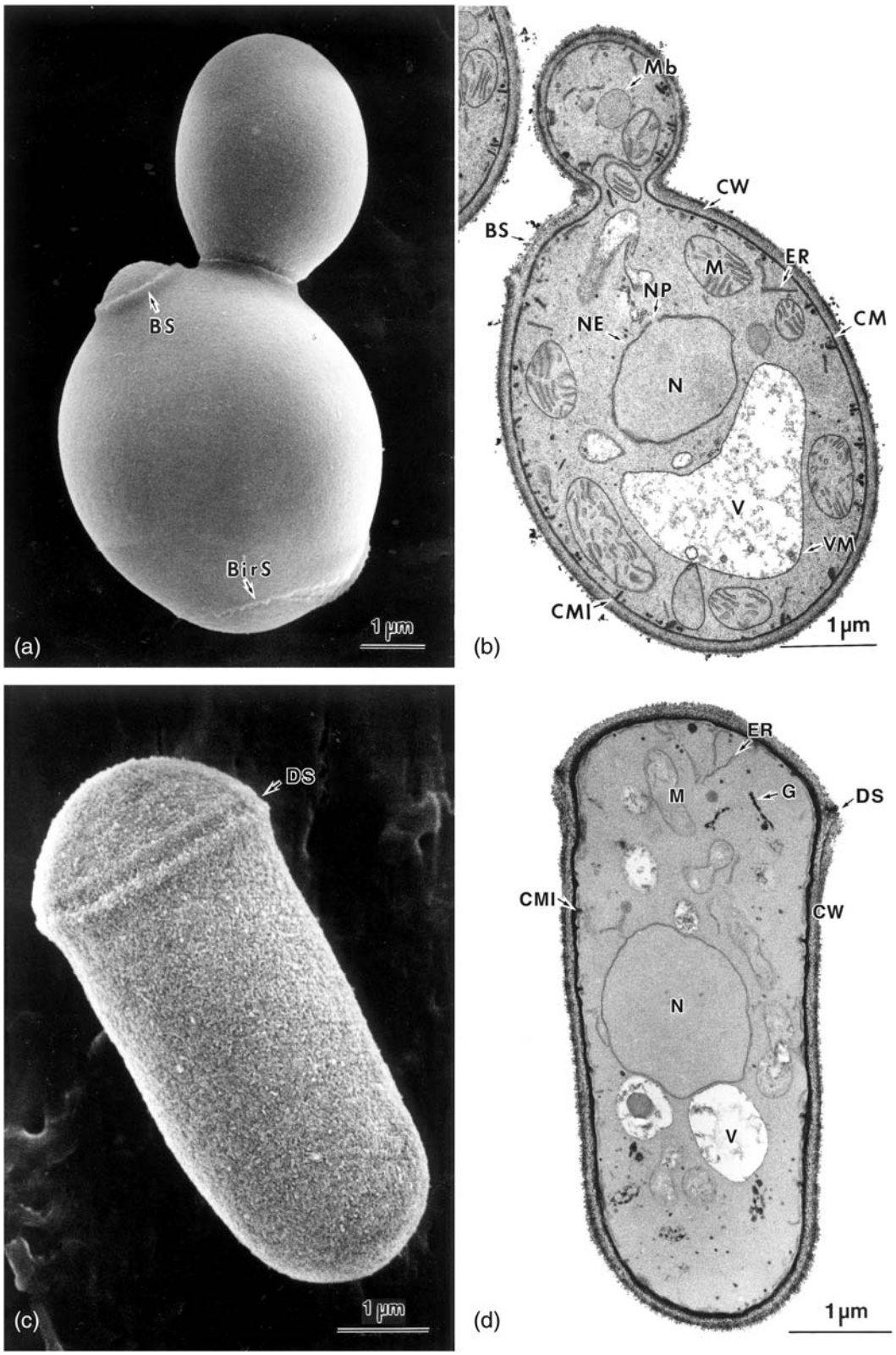

Fig. 1. General features of yeast cells. Budding yeast, *Saccharomyces cerevisiae* (a) and *Candida albicans* (b), and fission yeast, *Schizosaccharomyces pombe* (c and d). (a and c) SEM images. (b and d) TEM images [9]. BS, bud scar; Bir S, birth scar; CM, cell membrane; CMI, invagination of cell membrane; CW, cell wall; DS, division scar; ER, endplasmic reticulum; G, Golgi apparatus; M, mitochondrion; Mb, microbody; N, nucleus NP, nuclear pore; NE, nuclear envelope; V, vacuole; VM, vacuole membrane. (Reproduced with permission from Elsevier).

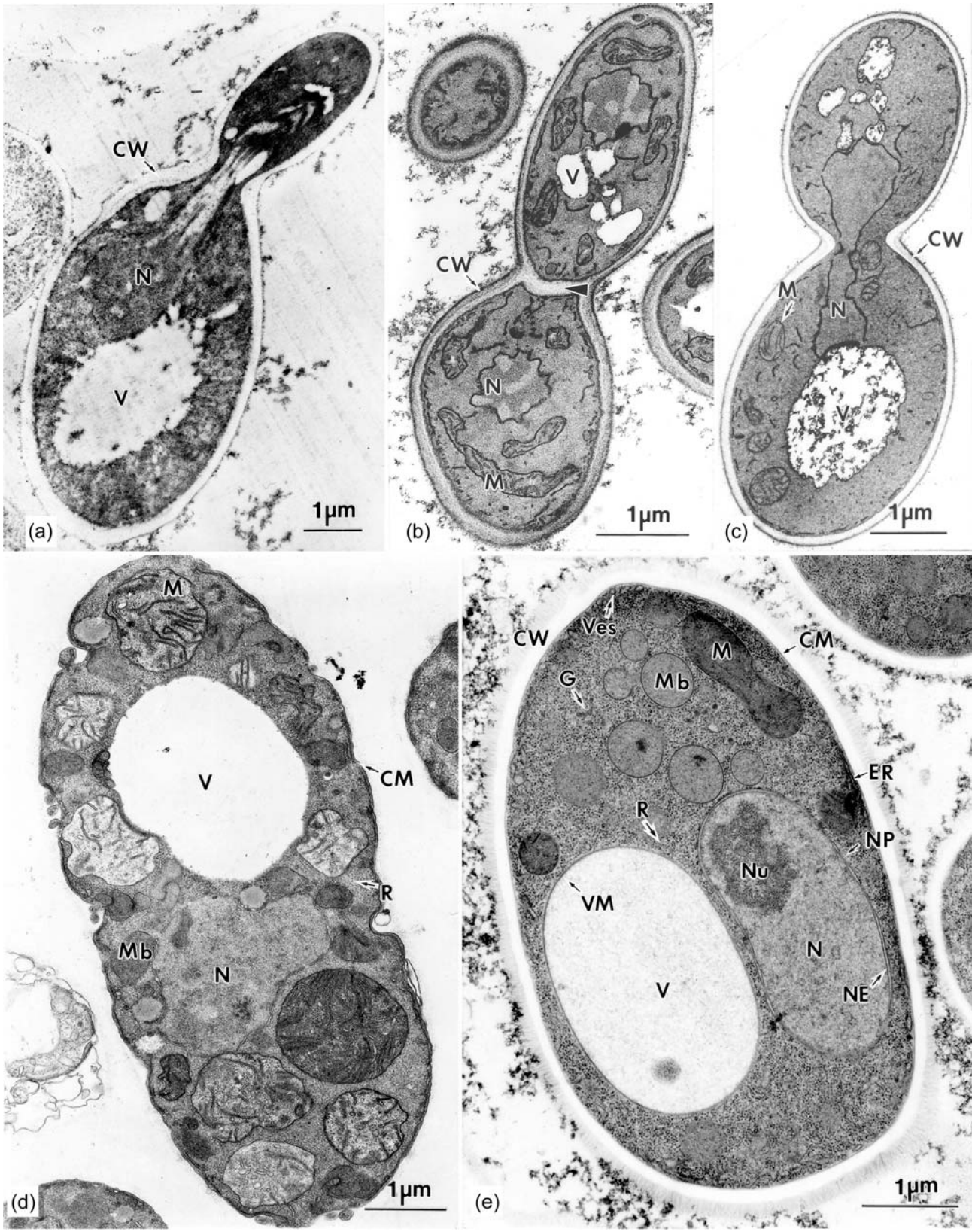

Fig. 2. Development of fixation methods of yeast. Images of $KMnO_4$ fixation taken in 1960 (a) and on 12 February 1967 (b), double fixation with GA and $KMnO_4$ on 17 November 1967 (c), GA-OsO_4 fixation of spheroplast in 1974 (d) and rapid freezing (sandwich method) and freeze substitution on 3 February 1985 (e) [9,66]. Nu, nucleuolus; Ves, vesicle; R, ribosome. (Reproduced with permission from Elsevier).

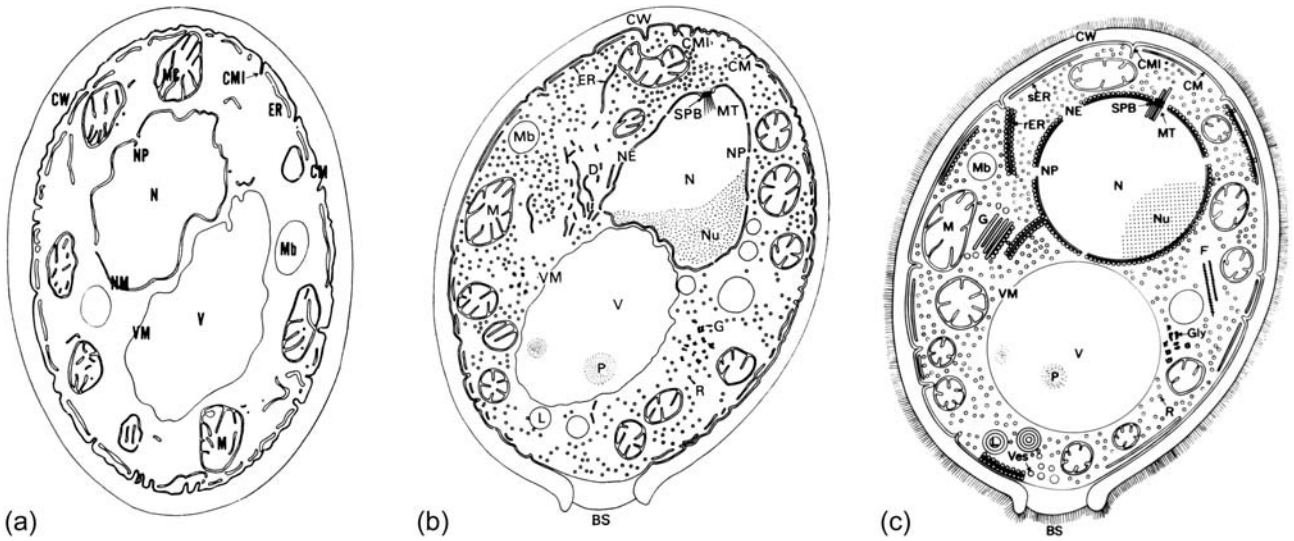

Fig. 3. Progress of ultrastracture model of yeast cell according to the development of the fixation method. (a) $KMnO_4$ fixation. (b) Double fixation with GA and OsO_4 fixation. (c) Rapid freezing and freeze substitution fixation with OsO_4. $KMnO_4$ destroys ribosomes and cytoskeletons. By digesting the cell wall, OsO_4 is able to penetrate into the cytoplasm and preserves the intracellular organelles, including ribosomes and cytoskeleton. Cells fixed by freeze substitution are spherical and all intracellular organelles are easily recognized. The surface of the cell wall is covered with a brash-like structure of the polysaccharides [9]. D, dictyosome (Golgi apparatus); rER, rough endoplasmic reticulum; sER, smooth endoplasmic reticulum; SPB, spindle pole body; MT, microtubule; P, polyphosphate; L, lipid; Gly, glycogen; F, actin fibril. (Reproduced with permission from Elsevier).

yeasts grown in *n*-alkanes [18]. Such microbodies in mammalian and plant cells have been identified as 'peroxisome' and /or 'glyoxysome', and catalase has been confirmed as the specific marker enzyme [19,20]. In the case of *Candida* yeasts growing in *n*-alkane as a sole carbon source, we found that the catalase activity is significantly higher than that growing in the usual carbon source, glucose, especially at the exponentially growing stage [21].

During the basic studies of the relationship between the appearance of microbodies and high catalase activity in *Candida* yeasts grown on *n*-alkanes, we established the isolation method of microbodies from the cells to investigate their ultrastructure [6].

The catalase activity in cells of various strains of *Candida* yeasts grown in *n*-alkane was markedly higher than that in the cells growing on glucose, ethanol or acetate. EM images revealed an abundant appearance of microbodies in the cells, and EM cytochemistry using 3,3-diaminobenzidine reagents confirmed the localization of catalase activity in the microbodies, as well as mitochondria [22–24].

Candida tropicalis cells, precultured on malt extract, contained microbodies scarcely, and showed very low levels of catalase activity. When the precultured cells were transferred to an *n*-alkane medium and incubated with shaking, the cell shape changed to the filamentous form over 16 h (Fig. 4a and b), and concomitantly the number and volume of microbodies and the catalase activity increased [22].

In the 1970s we wondered why microbodies gathered or aggregated with each other even there was enough space in the cytoplasm (Fig. 4a–d) [22]. In connection with this, a distinct structure was observed in the area where two microbodies touched each other, which we termed a 'zipper-like structure' (Fig. 4f–h). The presence of this structure was also confirmed by the freeze-fracture technique (see Supplementary data) [25]. This structure may cause aggregation of microbodies at the early stage of biogenesis, and may be concerned with the physiological stability of organelles or the efficiency of metabolism. Recently, the coiled-coil protein VIG1 has become to be essential for tethering vacuoles to mitochondria during vacuole inheritance of *Cyanidioschyzon merolae* [26]. Similar molecules to VIG1 may concern in association of microbodies. In recent years, in *Aspergillus oryzae*,

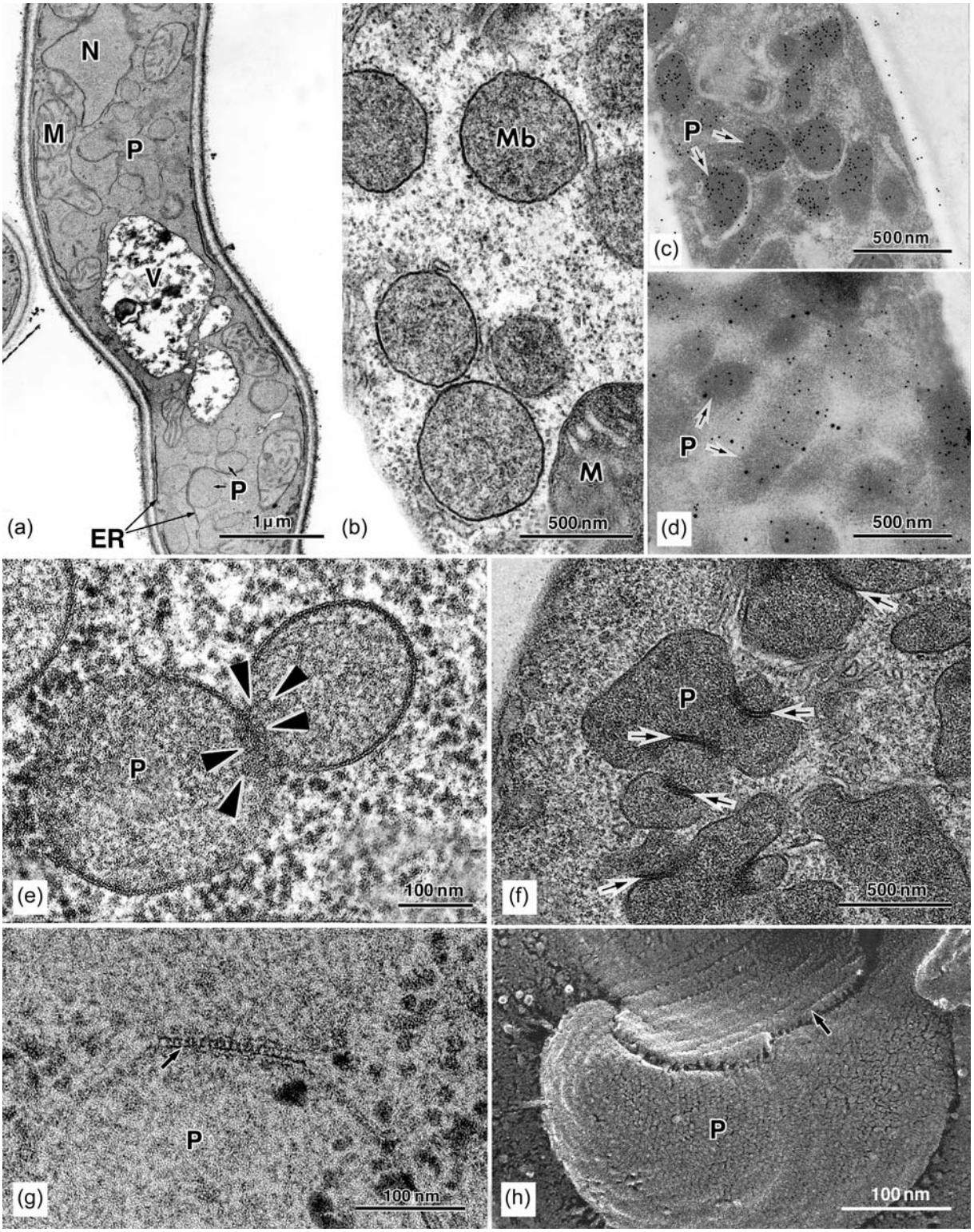

Fig. 4. Microbodies of *C. tropicalis*. Cells grown in hydrocarbon as a sole carbon source change to a filamentous shape and microbodies appear profusely. GA-$KMnO_4$ (a) and GA-OsO_4 (b) fixed cells. Localization of T-I (c), and T-I and T-III (d) by IEM. Small and large colloidal gold particles indicate T-I and T-III, respectively. (e) Dumbbell-shaped microbodies. (f) Joined microbodies. Zipper-like structure (arrow) observed by a thin section (g) and a freeze fracture replica (h). P indicates peroxisome (h, see Supplementary data).

the new function of peroxisome participating in the Woronin body formation has been reported [27].

Biogenesis of microbody

There are several hypotheses about the origin of microbodies. De Duve proposed that these organelles are derived from a dilated region of ER [28], although many of the published micrographs failed to demonstrate a direct continuity between the membrane of the nascent microbodies and the ER membrane. Our observation in the 1970s suggested it seems most likely that yeast microbodies would originate from preexisting microbodies. This assumption may be supported by the fact that microbodies exist as aggregations in cells incubated for 6–8 h on the *n*-alkane medium, and in 46 h-old cells the cytoplasm is filled with the organelles [22]. In contrast, ER does not arise in cells during the early incubation period with the *n*-alkane medium. Recently, dumbbell-shaped microbodies were observed which had electron dense particles inside a constricted area (10 nm ϕ, arrows in Fig. 4e) in 2.5 h-cultured cells. It is possible that these particles are involved in the control of the division of microbodies [29,30]. Furthermore it has been shown that two daughter microbodies arise by binary fission of the preexisting microbody in alga *Cyanidioschyzon*, which contains one microbody per cell [31].

On the other hand, in yeast *Saccharomyces cerevisiae*, peroxisome fuses distinct vesicles derived from the ER [32], indicating that research of peroxisome biogenesis now reopens the discussion of the participation of ER [33,34]. In near future the process of multiplication, segregation and breakdown of peroxisome will be elucidated by means of the latest visualization techniques: UHR EM and super resolution fluorescence microscopy.

Enzymes in microbodies of *Candida tropicalis*

We determined by immunoelectron microscopy (IEM) that the microbodies of *C. tropicalis* cells grown in *n*-alkane included thiolase, acetyl CoA (T-I) and 3-ketoacetyl CoA thiolase (T-III), which are enzymes for β-oxidation of fatty acid. The T-III locates specifically in the microbodies, whereas T-I was detected both in the cytoplasm and microbodies (Fig. 4c and d). These results were consistent with the biochemical data based on subcellular fractionation, indicating that the yeast β-oxidation system operates efficiently only in the microbody. Other peroxisomal enzymes, acetyl-CoA oxidase, catalase, cartinin acetyltransferase, isocitrate lyase (ICL) and malate synthase, were also detected in microbodies [35,36].

The ICL gene of *n*-alkane utilizable yeast *C. tropicalis* could be expressed in *S. cerevisiae* MT8-1 cells grown on an oleic acid medium, and the enzyme proteins transported into the microbody. To identify the signal sequence responsible for the proper subcellular location of *C. tropicalis* ICL (CT-ICL) in *S. cerevisiae*, the localization of truncated mutants of CT-ICL were examined by IEM. Three amino acids residues at the C-terminal end were not an essential sequence for the location in the peroxisomes. In cells expressing the internal region of the CT-ICL gene, the expressed polypeptides did not transport to the peroxisomes; rather, the polypeptides were mis-targeted to mitochondria or formed a protein aggregate body (PAB) in the cytoplasm [37]. PAB is now generally termed ‘aggresome’.

Composite crystalloid in the microbody of methanol utilizable yeast *Candida boidinii*

In the course of the studies of the physiology of methanol utilizing yeasts, *Kloeckera sp.* no 2201 (also known as *C. boidinii*), microbodies of small size, were found in cells grown in a glucose medium, transferred into methanol medium and then incubated for 2 h. After 4 h of cultivation, 5–6 microbodies were observed on the section of the cell (Fig. 5a). Although the number did not change during prolonged cultivation, their size increased with the passage of cultivation time. The microbodies were successfully isolated by means of sucrose gradient centrifugations from the methanol-grown cells [38], and microbody-specific enzyme activities were detected in the fraction by biochemical techniques. The activity of catalase and alcohol oxidase, the key enzymes of methanol oxidation, was also found in the fraction throughout the cultivation period [39].

The ultrastructure of microbodies in methanol-grown cells differed from that of hydrocarbon utilizing cells, and they have a lattice structure (Fig. 5b). The use of a cryo-sectioning technique, together

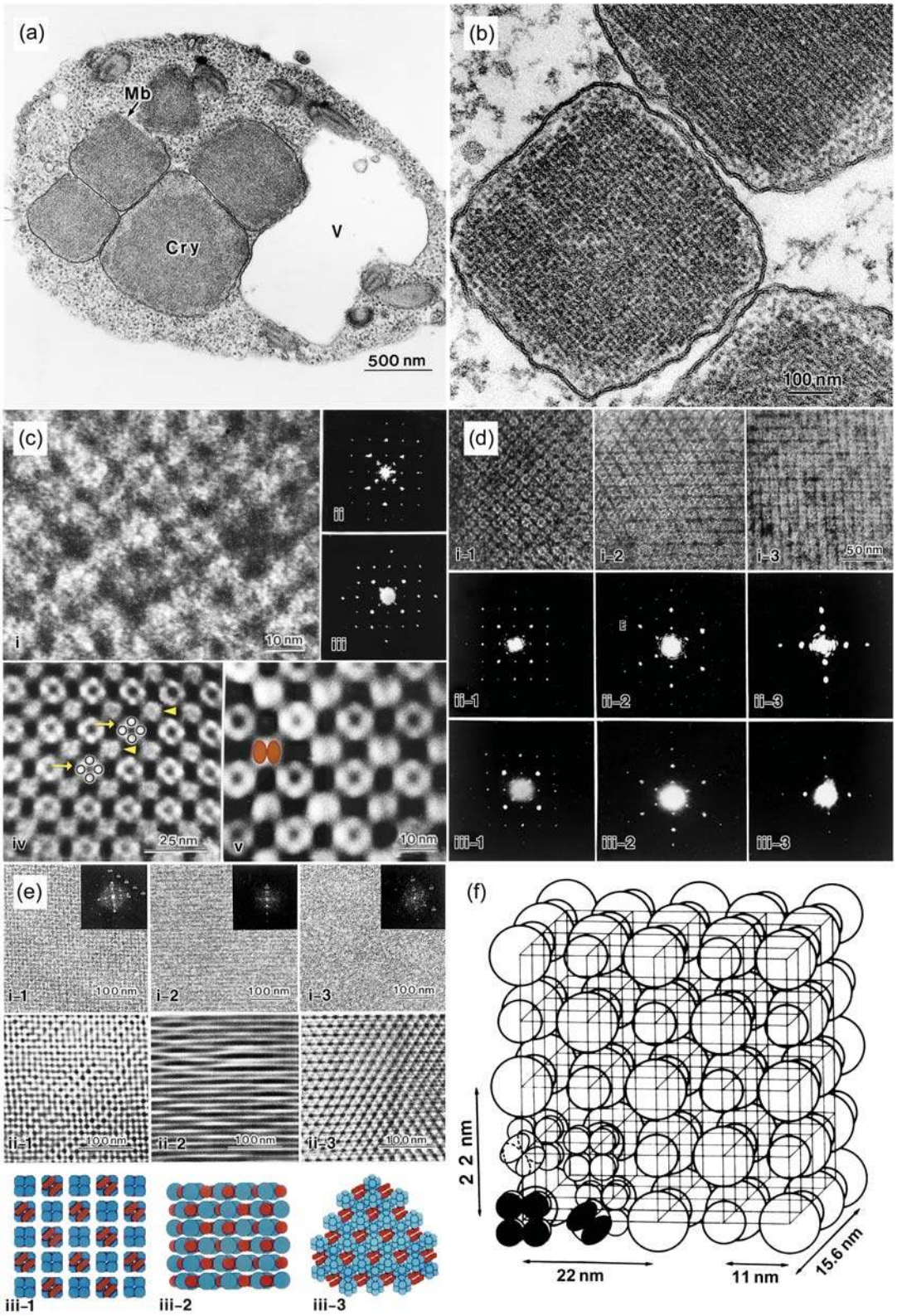

Fig. 5. Microbodies of *C. bodinii*. (a) The cell grown in methanol as a sole carbon source has few microbodies containing crystalloid inside. (b) Lattice structure of crystalloid. (c) Microbody crystalloid. (c–i) Negative staining image with uranium acetate. (c–ii) Optical diffraction. (c–iii) Electron diffraction. (c–iv) Malti-81 times superimposed images showing four sub-units (circle) in the large particle. (c–v) Optical filtering image showing four subunits in the large particle and two sub-units in the small particle (red). (d, i1–i3) Three tilting images of crystalloid. (d, ii1–ii3) Optical diffraction. (d, iii1–iii3) Electron diffraction. (e) Reconstructed images. (f) 3D model of crystalloid [41–47]. Reproduction from references [42,44]. Cry, crystalloid. (Reproduced with permission from American Society for Microbiology).

with electron diffraction, optical diffraction and filtering and computer simulation, determined the intrinsic structure of the crystalloid. The activity of alcohol oxidase and catalase was found uniformly in the crystalloid, using electron probe microanalysis [40] of cryo-sections, as well as by EM cytochemistry [41–47].

Profiles of the microbody crystalloid in the cryo-sections with negative staining, which was a popular technique for detecting the finest structure at that time, were classified into three types: tetragonal, hexagonal and rectangular lattice (Fig. 5d, i1–i3). When a figure of Fig. 5c–i was superimposed 81 times (which was the old analytical method), large and small particles were found (yellow arrow and arrowhead, respectively in Fig. 5c–iv). The large particle was composed of 4 subunits. However, the number of subunits in small particles was impossible to determine by this method. Then, the particle was analyzed by an optical filtering technique [48], which was the most advanced technique at that time, and two small subunits were found in the small particles (Fig. 5c–v, red).

Their optical diffraction (Fig. 5d, ii1–ii3) and also electron diffractions (Fig. 5d, iii1–iii3) revealed that the crystalloid has a cubic structure. By tilting experiments, one of the three profiles of the lattice was converted to another (Fig. 5d, i1–i3). Optical diffraction images (Fig. 5d, ii1–ii3) clearly showed that the lattice was composed of two types of particles, with different diameters of 10 and 7 nm, which were arranged alternately. Computer simulations of tilting images of the crystalloid conclusively showed that the crystalloid comprises composite crystals of two particles, and that large and small particles were composed of eight (blue) and four (red) subunits, respectively (Fig. 5e-iii). Large particles seemed to consist of alcohol oxidase molecules, while the small particles were presumably made up of catalase according to their molecular weight. We proposed the 3D model of the microbody crystalloid (Fig. 5f) [45]. The distance between particles was 11 nm with a unit cell length of 22 nm, and the shortest distance between two large (or small) particles measured 15.6 nm. They located alternately to make up the composite crystals, the same as the structure of rock salt. These composite crystals can participate most effectively in methanol oxidation in the cell.

Mechanism of cell wall formation

Since the protoplasts of *Schizosaccharomyces pombe* can completely regenerate cell walls to revert to normal cells in liquid media, the regenerating process is a good model system to examine a *de novo* process for cell wall synthesis: (i) initiation of the cell wall, (ii) formation of microfibrils, (iii) deposition of an amorphous wall substances and (iv) involvement of the actin cytoskeleton.

Summary of the cytoskeletal changes during cytokinesis of *Schizosaccharomyces pombe*

Fission yeasts are useful model organisms for research into the cell division cycle [4,49,50]. In the 1980 and 1990 s, the behavior of the cytoskeleton during the yeast cell cycle was intensively studied in many laboratories, including the author's [51–59].

We proposed that the actin cytoskeleton plays a leading role in the formation of the cell wall through studies, starting in 1989, of cell wall formation and the behavior of filasomes [60,61] using a fluorescence microscopy. We also found that prior to septum formation, actin localized as if to lead invagination of the cell membrane, and formed an actin ring with the progress of septum expansion [14,62,63]. The actin cytoskeleton may play the role of conductor in the cytokinesis [64–67]. Figure 6 summarizes the cytoskeletal changes through the cell division cycle in *S. pombe* [51–59,68,69].

Development of UHR-LVSEM

To visualize details of a regenerating cell wall, we developed an improved UHR FESEM S-900LV, collaborating with Hitachi Co., which gives us better resolution at low beam energy (~5 kV or below) with small aberrations of the objective lens and a shorter working distance [70,71]. This modified in-lens FESEM S-900, referred to here as S-900LV (commercial model SEM S-900H), is a type of UHR LVSEM, which enables us to observe directly the surface topographs of uncoated biological samples with maximum fidelity (Fig. 7) [72].

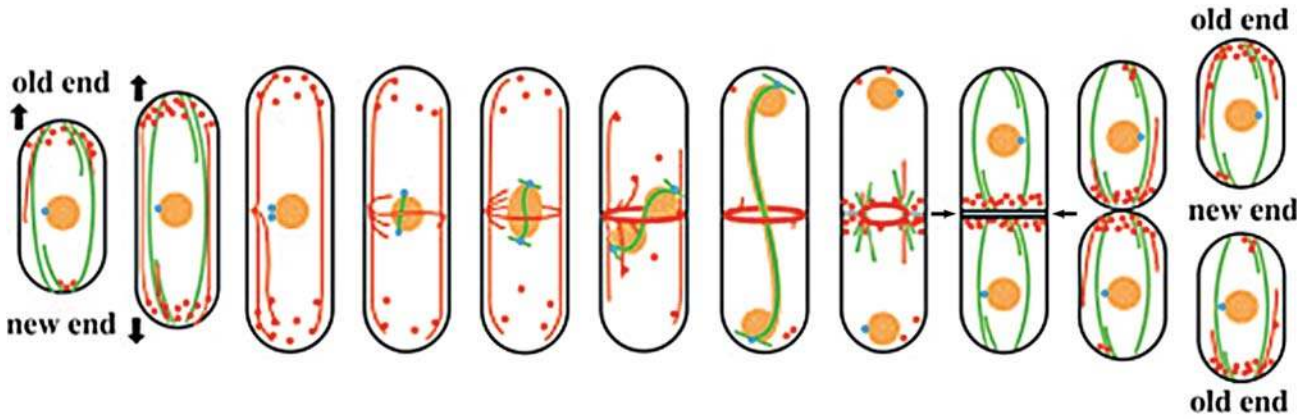

Fig. 6. Summary of the cytoskeletal changes during cytokinesis of *S. pombe*. Orange circle, nucleus; Red line, ring and dot, F-actin cable, contractile ring, actin patch, respectively; Green line, cytoplasmic microtubules and spindle microtubules; blue dots, spindle pole body; gray (arrows) and black line, primary and secondary septum,respectively. Reproduced from reference [51–59, 68, 69].

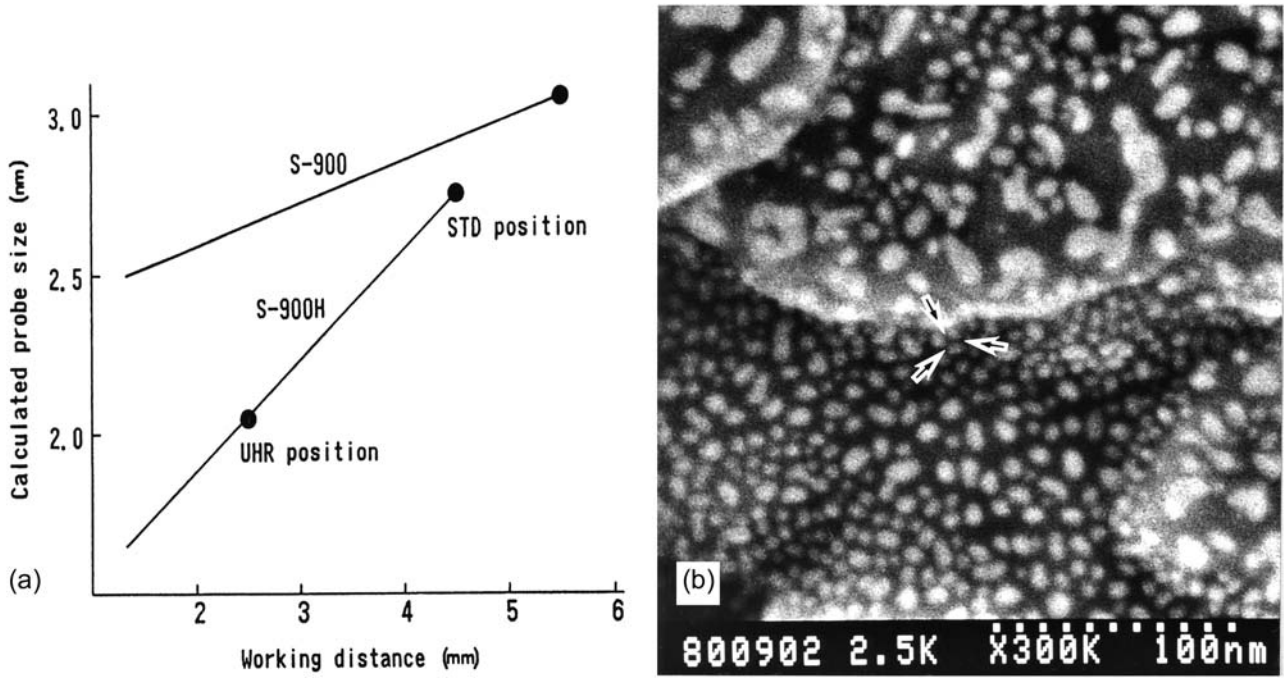

Fig. 7. Resolution of S-900 LV. (a) Probe size calculated at 1 kV and different working distances (WD). 5 kV or below is used for UHR position at 2.5 mm WD. (b) Arrows indicate the most narrowest gaps between gold particles (bright spots) settled on vacuum-evaporated magnetic tape, at 1 kV and an original magnification of ×300 000 [72].

Dynamics of the ultrastructure during cell wall formation in *Schizosaccharomyces pombe* observed by SEM and TEM

Using a UHR LVSEM S-900 LV and S-900, we can study the ultrastructure of regenerating cell walls of *S. pombe* protoplasts with uncoated or slightly coated [73] surfaces, respectively. Just after digesting the cell wall of the cylindrical *S. pombe* cells with Novozyme 234, no cell wall material was seen on the surface of the round shaped protoplast (Fig. 8a). The absence of staining with calcofluor confirmed that the surface of freshly prepared protoplasts was free from cell wall materials, glucans and α-garactomannnan [59]. TEM images of thin sections also confirmed the absence of the remnants of old wall materials on the surface [74]. Many invaginations of the cell membrane, which is unique to *S. pombe*, were found on the surface.

After 10 min incubation, a portion of the surface accumulated invaginations (Fig. 8b, →), and at 1.5 h

fibrous materials appeared at the area (Fig. 8c, →). After 5 h, fibrous network covered the whole surface of the protoplast, and the shape of the protoplast changed to the elongated form (Fig. 8e). The microfibrils twisted around each other and developed into thick fibrils forming flat bundles.

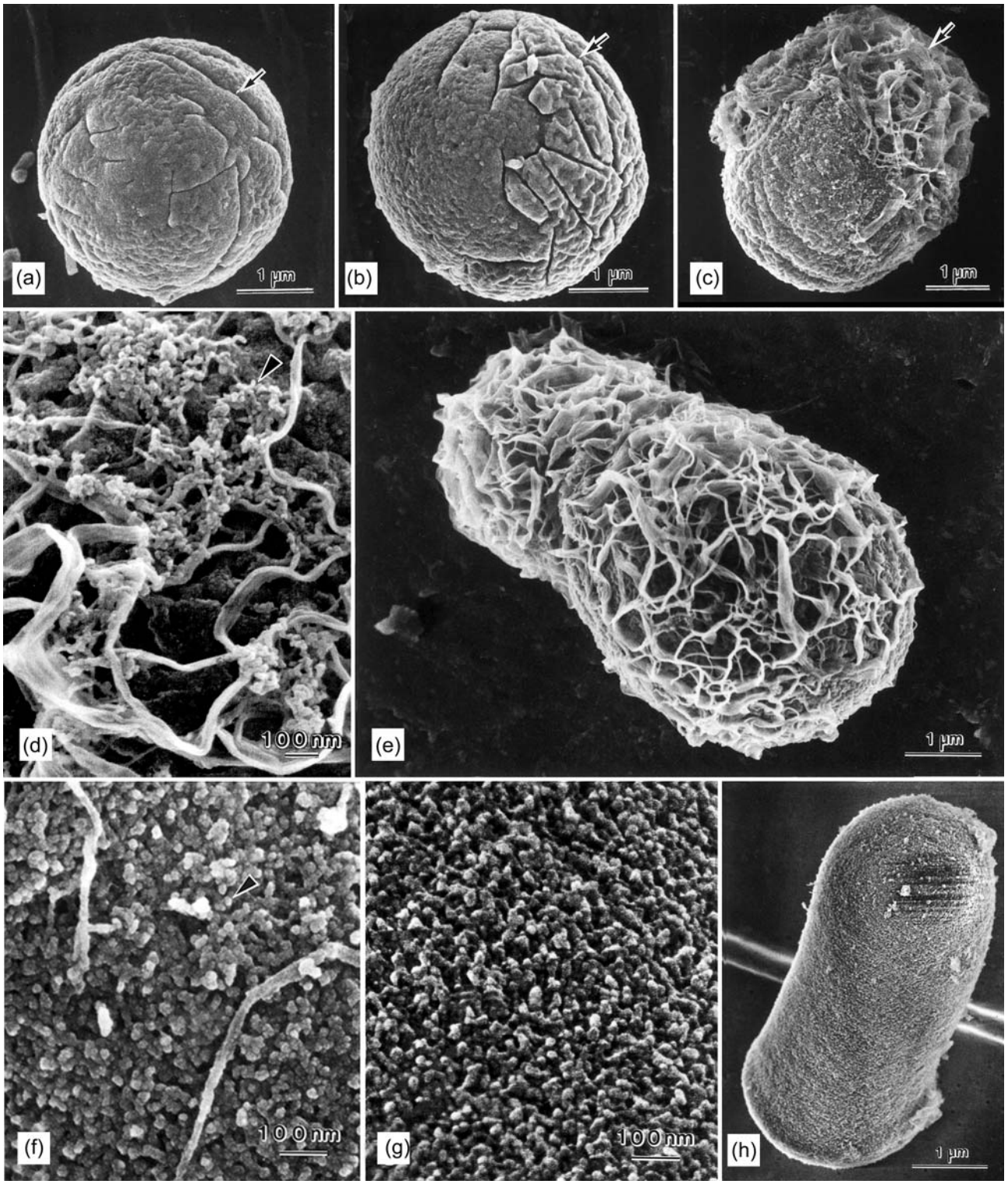

Fig. 8. Regeneration processes of reverting protoplast. The specimens were slightly coated with a <2 nm layer of platinum-carbon at 2×10^{-7} Pa and 10°C in a Balzers 500 K with the electron gun. (a) Protoplast. Cell wall regeneration process after 10 min (b), 1.5 h (c), 3 h (d), 5 h (e), 10 h (f) and 12 h (g and h). (i), Architecture of fibrous network (uncoated specimen). (j) Detection of α-galactomannan using lectin-conjugated gold particles (40 nm, coated with carbon). See references [72,73,75,79].

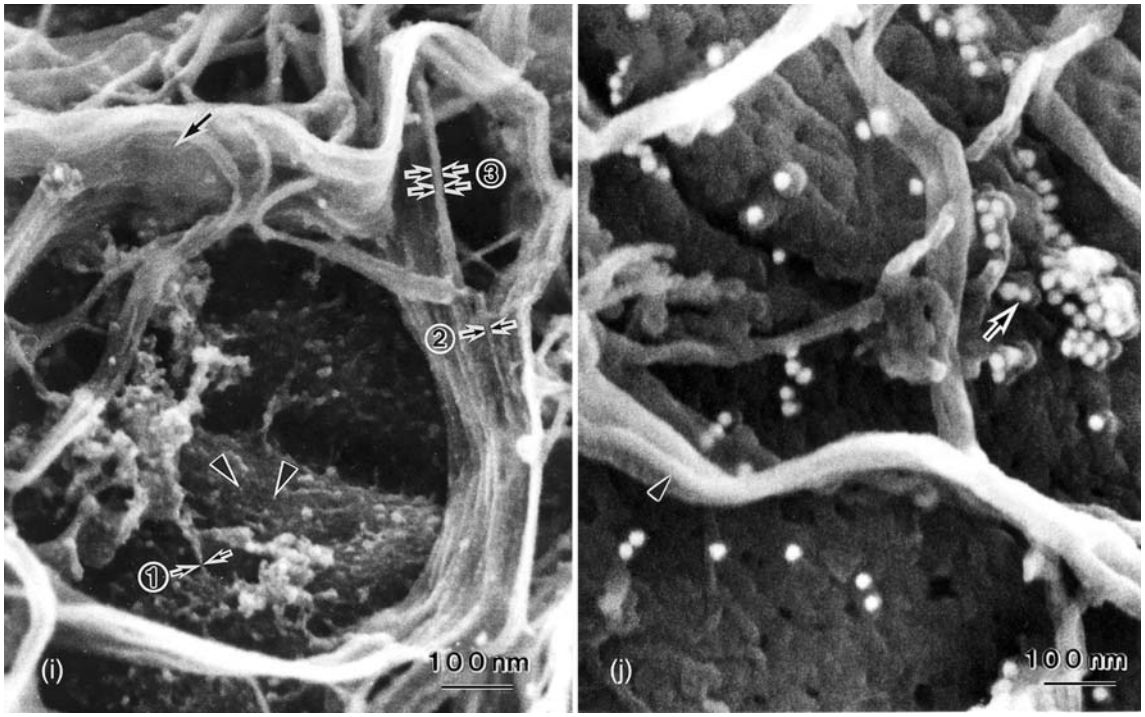

Fig. 8. *Continued*

Intrafibrillar spaces were gradually filled with particles (Fig. 8d, arrowhead). After 10 h, the granular materials filled up intrafibrillar spaces on the surface (Fig. 8f). Finally, after 12 h the complete cell wall was regenerated (Fig. 8g and h) [75].

In the cell-free system using isolated cell membrane of *C. albicans* and the negative staining method, secreted particles (2 nm ϕ) subsequently converted to microfibrils ~4 nm thick [76]. Uncoated UHR LVSEM images of the regenerating protoplast showed scattered particles, ~3 nm ϕ (arrowhead) and 2 nm thick (①) microfibrils on the cell surface (Fig. 8i). These microfibrils may be joined end to end, twisted around each other, attached side-by-side to 8 nm thick (②) fibrils, and then developed to a ribbon shaped network ~16 nm thick 16 nm thick (③). The ribbon shaped structures further contacted side by side and finally formed diversified structures with various width and length, up to 200 nm wide and 1 μm long (arrow) [72]. SEM images of microfibrils and ribbon shaped structures shown here were similar to TEM images of a negatively stained specimen of the reverting protoplast for 3 h (Fig. 10a) [9,72,75].

Identification of cell wall components

Bundles formed on the surface of reverting protoplasts were cleaved into small pieces when the protoplasts were treated with β-1,3-glucanase for 2 h (Fig. 10a and b) [9,72] and completely digested with longer treatment. Furthermore, fibrous networks are not formed on the protoplasts in the presence of aculeacin A, an antifungal antibiotic and a potent inhibitor of β-1, 3-glucan synthesis [76–78]. Immunogold signals against for β-1,3-glucan were detected on IEM (Fig. 10d and e arrows). Thus, fibrous structures are composed of microfibrils of β-1,3-glucan as in a budding yeast cell wall [76,78]. By using gold-labeled lectin, α-galactomannan was detected on particles locating in the intrafibrillar space of the reverting protoplast for 3 h (arrowhead in Fig. 8d, f and j) [79]. The intrafibrillar spaces were filled with the particles after 12 h (Fig. 8g) indicating α-galactomannan was also an ingredient of the cell wall.

In addition to β-1,3-glucan, it was found by NMR spectroscopy [80] and IEM using an antibody against α-1,3-glucan that the *S. pombe* cell wall included α-1,3-glucan. Most of all, the α-1,3-glucan

distributed just outside the cell membrane, supporting previous reports that the α-glucan is synthesized on the cell membrane [81]. Recently we also detected Mok 1p, the protein of α-1,3-glucan synthetase, locating on the cell membrane. Mok 1p moves from the cell tip to the medial region during the cell cycle [14]. These results show that α-1,3-glucan is required for the primary step of glucan bundle formation in new cell wall synthesis during vegetative growth.

Based on the experiment using anti- β-1, 6 glucan antibodies, we proposed that β-1, 6 glucan in a highly branched form is also an ingredient of the cell wall. However, such β-1, 6 glucan was not recognized on the Golgi body [66,82]; rather, they existed in the cytoplasm and beneath of the cell membrane. From these results and the fact that the low molecular α-1,3-glucan was transported through the secretory pathway to the cell membrane where the synthase located, and then synthesized into higher molecules, it was speculated that linear β-1, 6 glucan was synthesized in the endoplasmic reticulum-Golgi system, and that highly branched structures were formed on the cell membrane (Fig. 9) [66,67,82]. Thus β-1,6-glucan, as well as α-1,3-glucan and β-1,3-glucan, is an ingredient of the cell wall of *S. pombe*. Those glucans and α-galactomannan are characteristic components of this yeast [83]. Throughout these experiments, we used antibodies against α-1,3-glucan, and highly branched β-1,6-glucan that we had prepared [80].

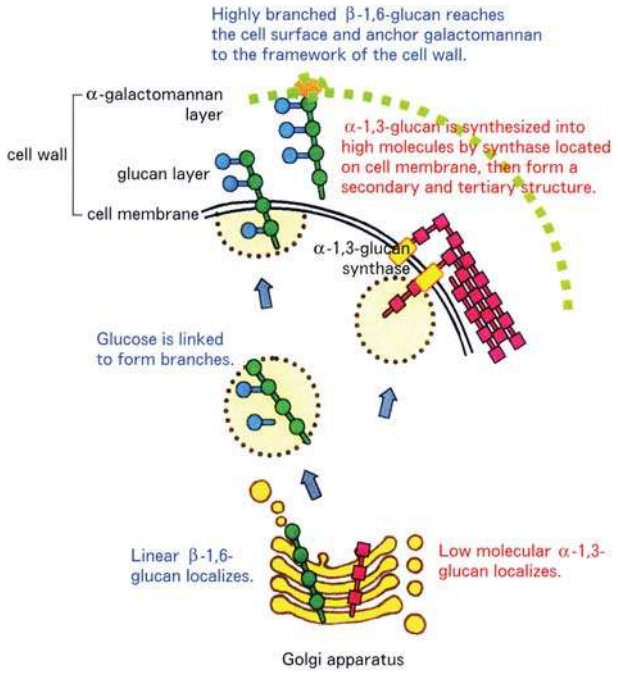

Fig. 9. Schema of secretion process of the cell wall glucans and α-galactomannan [67].

Treatment with ruthenium tetroxide (RuO_4) [84–86] after conventional fixation provides clear TEM images of glucan fibrils and the outer surface of the cell membrane with high electron density [61]. Also, filasomes (Fig. 10i), Golgi apparatus and secretory vesicles are clearly visible in the cytoplasm. The regenerated fibrils stained with RuO_4 show the twisted (Fig. 10f), separated (Fig. 10g), anchored (Fig. 10h) and ring- or canal-shaped forms (Fig. 10c and d) [9]. The finest regenerating glucan fibril is 1.0–1.5 nm in diameter (Fig. 10a arrow, Fig. 10c, →←), which is slightly less than that of the SEM image.

Just beneath the cell membrane filasomes are easily identified (Fig. 10i) by heavy staining with RuO_4 [61]. They are 100–300 nm in diameter and consist of one microvesicle (35–70 nm in diameter) and fine filaments surrounding the vesicle [65]. The location of filasomes in reverting protoplasts coincides with the site where F-actin patches exist [65]. It seems that filasomes may contribute to transporting the cell wall materials from the cytoplasm to underneath the cell membrane.

Mechanism of cell wall formation and 3D images of intracellular structure during regeneration of the protoplast

The cell wall and septum are abnormal in actin point mutant *cps8*, and the distribution pattern of the actin cytoskeleton differs from wild-type [87,88]. In the mutant cells, the development of crosslinks between β-1,3-glucan fibrils was defective, and the intrafibrillar space on the reverting protoplast surface was not filled with amorphous particles composed of α-galactomannan [89]. In the wild type cells, formation of the fibril network was completely inhibited in the presence of 40 μg ml^{-1} cytochalasin D, and this inhibition was reversible [59]. These results suggest that the actin cytoskeleton may control secretion of cell wall materials such as α-galactomannan. In addition, the actin cytoskeleton requires localization of α-1,3-glucan

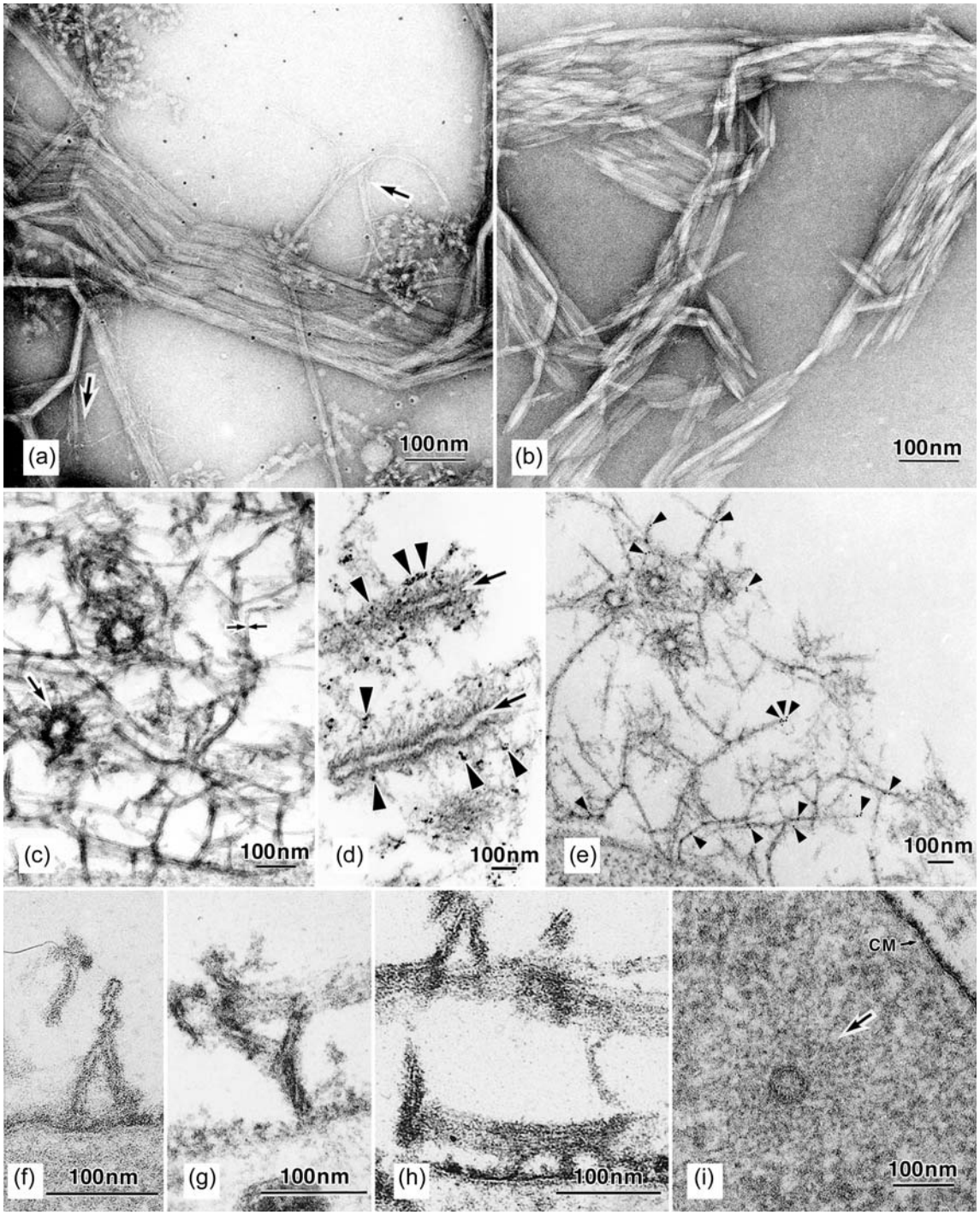

Fig. 10. β-1,3-glucan fibrils in cell wall and filasome. Surface materials from reverting protoplast for 3 h were negatively stained after treatment with β-1,3-glucanese for 0 h (a) and 2 h (b). (c) Thin section images of the network of glucan fibrils. (d and e) IEM images showing the *in situ* localization of β-1,3-glucan (arrowhead). One nm colloidal gold was visualized by enhanced method. Thin fibril of 1–1.5 nm in diameter (arrows in a and →← in c), and ring-shaped (arrow in c) or canal-shaped forms (arrow in d). (f–h) Development of glucan fibrils. (i) Filasome (arrow) appearing beneath the cell membrane. Specimens were stained with RuO_4 (c–i) [9]. (Reproduced with permission from Elsevier).

synthase to the site of growth and plays an essential role in cell morphogenesis [90].

Protoplast treated with periodic acid-thiocarbohydrazide-silver protein staining for polysaccharides (PATAg) shows a higher electron density of Golgi bodies [74]. The intracellular secretion machinery, especially the Golgi apparatus and secretory vesicles, was analyzed by 3D reconstruction from 40 to 80

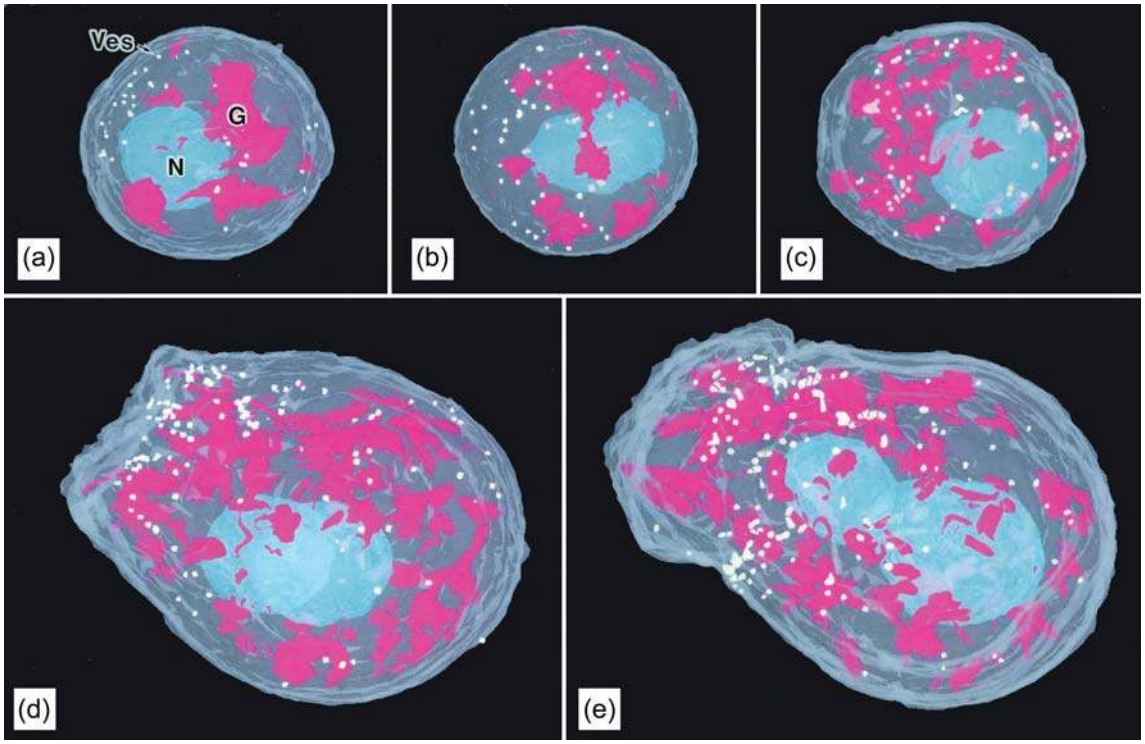

Fig. 11. 3D reconstruction of reverting protoplast forming cell wall. The whole serial sections of reverting protoplast at 0 min (a), 10 min (b), 1.5 h (c), 3,0 h (d) and 5 h (e). Blue, pink, gray and white dots indicate nucleus, Golgi apparatus, cytoplasm and secretory vesicles, respectively [74]. (Reproduced with permission from Elsevier).

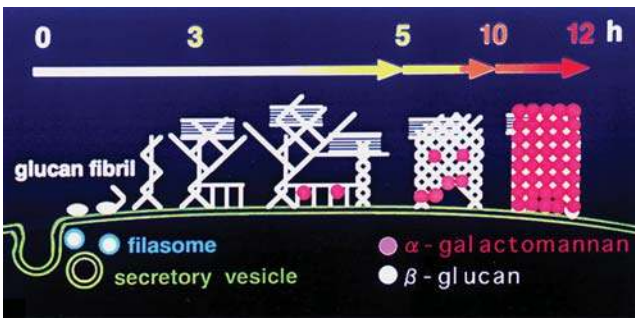

Fig. 12. Schema of cell wall formation of fission yeast protoplast. Numbers indicate reverting time of the protoplast [9]. See Dynamics of the ultrastructure during cell wall formation in *Schizosaccharomyces pombe* observed by SEM and TEM, Identification of cell wall components, Mechanism of cell wall formation and 3D images of intracellular structure during regeneration of the protoplast Sections. (Reproduced with permission from Elsevier).

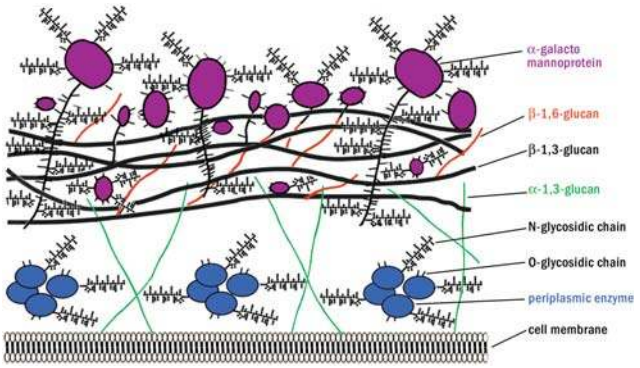

Fig. 13. Model of molecular composition and structure of cell wall of *S. pombe*. The cell wall consists of two layers. The inner layer provides cell wall strength, and is made from β-1,3- and β-1,6-glucan, and α-1,3-glucan. The outer layer consists of α-galactomanno-proteins and determines most of the surface properties of the cell. (Reproduced by courtesy of Professor F.M. Klis) [9, 91, 98]. (Reproduced with permission from Elsevier).

serial sections of protoplasts stained with PATAg at five distinct reverting stages (Fig. 11). The total volume of reverting protoplast increased by 3.8 and 4.3 times at 3 and 5 h, respectively, and the volume of Golgi apparatus at the corresponding stages increased 2.3- and 2.5-fold, respectively. The number of secretory vesicles also increased markedly by 3.4 and 5.8 times, respectively. Filasomes may correlate with this secretory system.

Combined data, obtained by using UHR LVSEM and TEM techniques, suggest the mechanism of cell wall formation in yeast as shown in Fig. 12 [9]. In addition, our data together with other studies [83,91–97] proposes the composition and structure of the cell wall of *S. pombe* (Fig. 13) [9,98].

Significance of the HPF technique in structural biology – with reference to a study of septum formation in fission yeast

HPF was first used as an alternative method of cryo-fixation in the 1960s, and has advanced since then. The commercially available unit is reliable with respect to its physical performance in yeast cells as well as plant tissues [99]. Cells of *S. pombe* were cryo-fixed by HPF using HPM 010 (BAL-TEC AG, Liechtenstein) under 210 MPa. They were observed at −140°C by Philips XL30 FEG and Hitachi S-4700 SEM, using the cryo-system Alto 2500 (Oxford), after cryo-cutting at −175 to −185°C

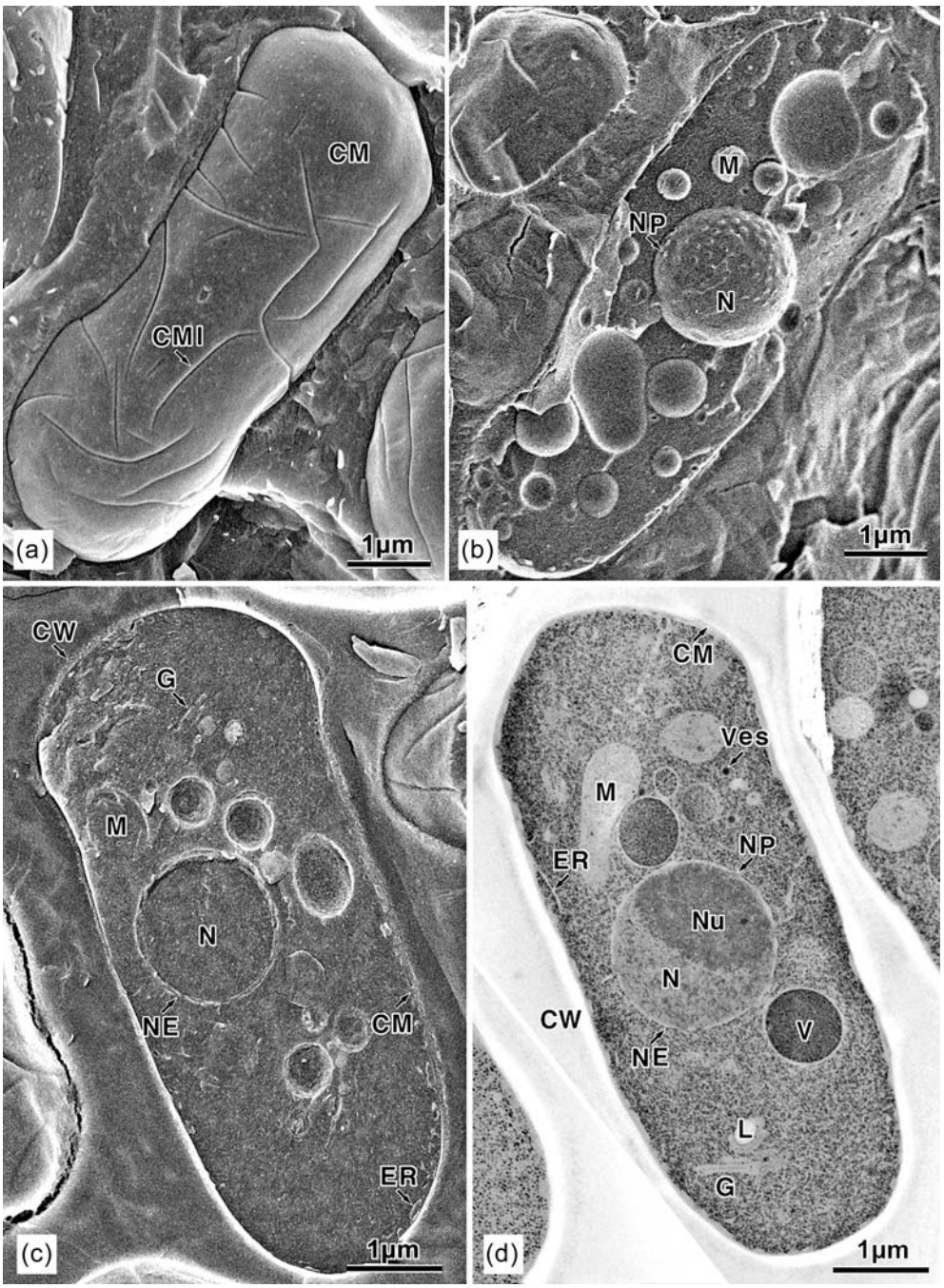

Fig. 14. ULT-LVSEM images of *S. pombe* cells cryo-fixed by HPF. (a) An outside image of a single cell showing PF face of the cell membrane. (b) An inside image of a cell. (c) An image of a cell cut in the central plane along with the longitudinal axis. (d) TEM image of a thin section [68].

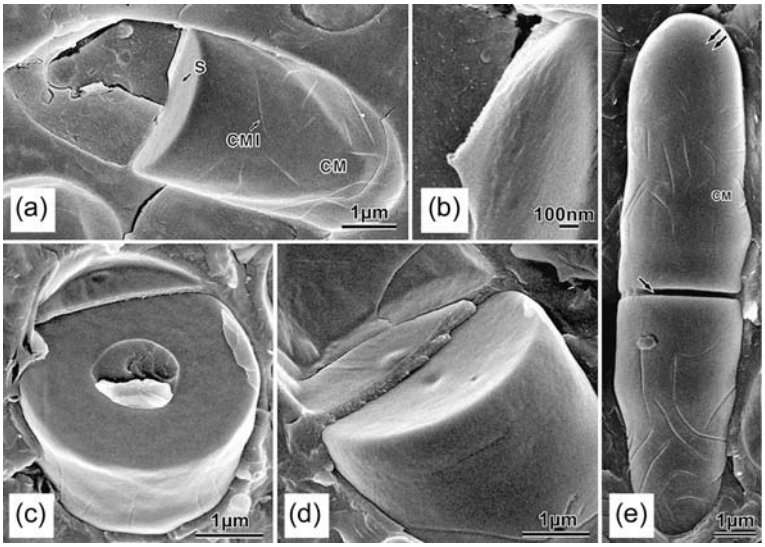

Fig. 15. ULT-LVSM images of the septum in dividing *S. pombe* cells. (a and b) The incomplete septum. (c) The PF face of the incomplete septum. (d) The PF face of the almost completed septum. Both sides of the PF face of the septum can be seen. (e) Bipolar growing cells (double arrows). There is no invagination on either side of the medial region (arrow) of the cell [4,68].

and magnetron spatter coating with platinum (2 mm). The high quality image by ultra-low temperature (ULT)-LVSEM showed an ultrastructure corresponding to the thin section of the same specimen, and 3D vision could observed from the outside and inside of the cell, allowing the stereo view of initial septum formation [68].

Figure14a and b show a fracture image of an outer side and the inside of a cell, respectively. A fracture image of a central plane along the longitudinal axis of a cell (Fig. 14c), closely resembles the thin-section image of the same HPF specimens (Fig. 14d). On the PF face of the cell membrane, invaginations found on the protoplast surface (Fig. 8a) are also observed (Fig. 14a). Fracture images of *S. pombe* cells forming septum during cytokinesis are shown on Fig. 15. Newly formed primary septum keeps expanding and is lined with secondary septum until the cytoplasm separates (see Fig. 6).

Throughout the septum formation, the immunogold labeled α-1,3-glucan molecules were observed on the expanding incomplete septum [14,68,69]. The α-1,3-glucan synthase Mok 1p is an essential enzyme for the synthesis of α-1,3-glucan. To analyze the behavior of Mok 1p during septum formation, frozen cells by HPF were prepared by freeze-fracture replica after SDS treatment and then labeled with antibodies (SDS-FRL) [100]. The

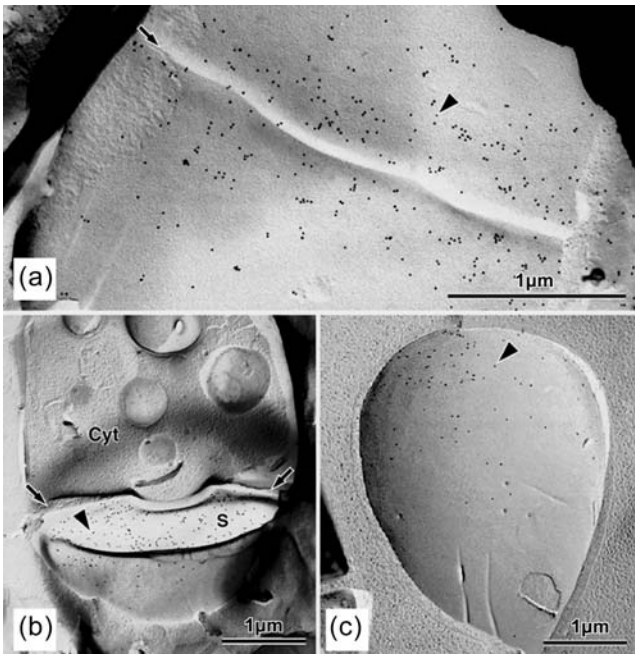

Fig. 16. SDS-FRL images of HPF *S. pombe* cells labeled with an anti-Mok1p antibody. (a) Mok1p (arrowhead) appears on the PF face of the cell membrane at the septum (arrow). (b) Mok1p also appears on the septum plane when its formation is complete. (c) Mok1p is localized on the tip of the swollen daughter cell (the new end) [68]. See Fig. 6. Cyt, cytoplasm.

immunogold-labeled Mok 1p molecules (arrowhead) accumulated on the cell membrane around the region where the septum was formed (Fig. 16a, arrow). Mok 1p were also localized on the membrane beneath complete septum (Fig. 16b,

arrowhead). After daughter cells separated, Mok 1p was observed on their swollen tip (Fig. 16c, arrowhead).

We now know the *in situ* localization and behavior of glucans, α-1,3-glucan, β-1,3-glucan, and highly branched β-1,6-glucan, during septum formation as well as in the cell wall of *S. pombe* [14,66,81].

Cryo-fixed specimens by HPF were also available for conventional TEM and IEM. The thin sections of cells showed a superior image of the fine structure of all subcellular organelles. The IEM images displayed *in situ* localization of glucans in *S. pombe* cells [66–69]. During septum formation β-1,3- and α-1,3-glucans were located in the invaginating primary septum, providing the first morphological evidence at the initial stage of septum formation. At this time, highly branched β-1,6-glucan was not detected, whereas other glucans were observed. Later, highly branched β-1,6-glucan also appeared on the secondary septum. Throughout the septum formation, actin was located just beneath the invaginated cell membrane and also accumulated at the medial region of the cell [63,64,67]. From these facts it is concluded that the actin cytoskeleton governs septum formation.

Very recently we found the essential function of α-1,3-glucan in the septation and cell separation during cell division [101].

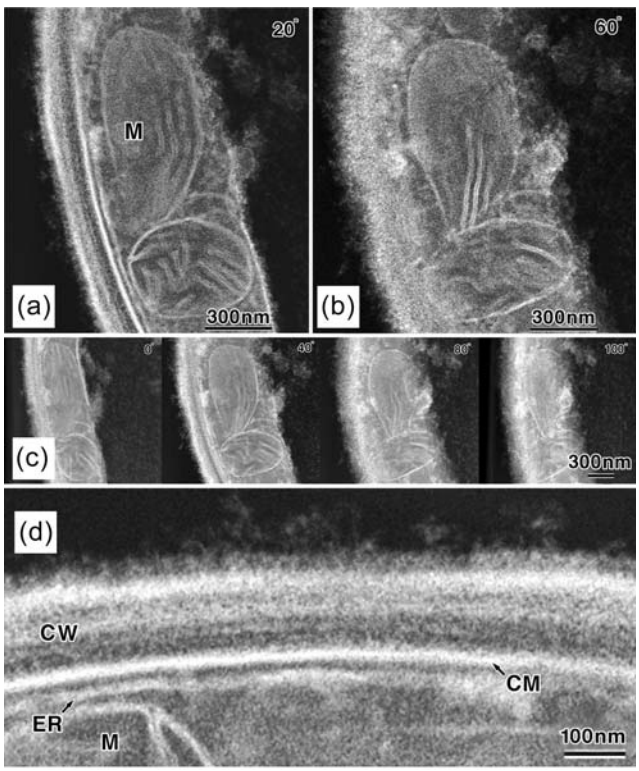

Fig. 17. The dark-field STEM images of a part of *C. tropicalis* cell wall by FIB micro-sampling [98].

FIB-scanning transmission electron microscopy (STEM) is useful for cell biology

To analyze the molecular architecture of cells, micro-sampling methods using an FIB, which are the main techniques for semiconductor device analysis, have been applied to yeast cells. This is the first case of applying FIB to the biological specimen [102].

The 0.3 μm thick specimen was obtained by milling with FIB, and the dark field image was observed by scanning transmission electron microscopy (STEM) (Fig. 17). Then, 3D images were constructed from 50 views taken by tilting 5° on a STEM. Six images are picked up and shown in Fig. 17a–c, and a clear image at high magnification in Fig. 17d [103–106]. On the outer surface of the cell wall, brush-like structures were recognized, clearly consisting of the presence of mannnoproteins (See Fig. 13), and fibrous structures were observed near the cell membrane side of the cell wall, consisting of glucan networks.

We tried to examine in more detail the cell wall architecture. The cell wall of *S. cerevisiae* was treated with acid after solubilizing the cytoplasm and prepared by FIB micro-sampling, and then the stereo images by STEM were taken at an original magnification of ×250 000. Fine fibrils were recognized inside the cell wall (circles in Fig. 18e and f) [98,105,106]. In addition, STEM is also useful for electron tomography of thick sections of biological specimens [107–109]. We succeeded determining the polarity of actin cytoskeleton modified with heavy meromyosin in cells of *S. pombe* that had been quite difficult to detect by usual IEM (Fig. 19) [98].

Future directions

I have reached the conclusion, from my long experience, that it is important to use the most suitable model system for each study. For example, I used

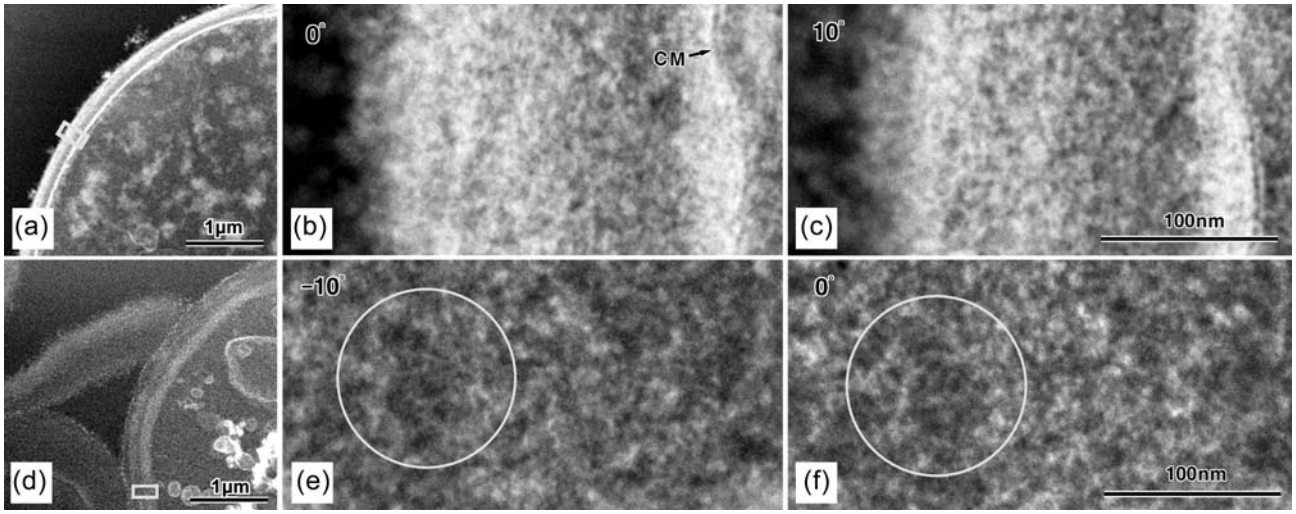

Fig. 18. Stereo-dark-field STEM images of cell wall of *S. cerevisiae*. Untreated (a–c) and treated (d–f) with acid after solubilizing cytoplasm. (a and d) A part of the cell wall. Areas indicated by the rectangles in (a) and (d) are enlarged in (b and c) and (e and f), respectively. Original magnification of ×250 000. Notice fibrils structures inside the circle [98].

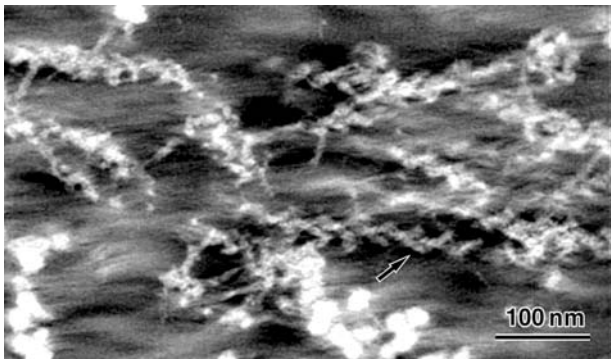

Fig. 19. Z-slice form of 3D-reconstructed volume of actin cabels (arrow) from dividing *S. pombe* cell and modified with heavy meromyosin by STEM taken by Dr K. Aoyama. The specimen was sliced by STEM-Tomography into 180 slices with 0.91 nm thickness. The image is 60th from the surface. Courtesy by Professor I. Mabuchi.

hydrocarbon- or methanol-utilizable yeasts to study the biogenesis of microbodies, and the regeneration system of protoplast was used to resolve the mechanism of cell wall formation. I found the best condition for conversion of the intact cells to protoplast at 100% yield even in a liquid medium, and could establish the system during the work. I also established some methods of analysis such as: (i) development of fixation, (ii) adoption of image reconstruction and analysis, even at the early period of EM, (iii) conception of rapid freezing by the sandwich method for yeasts, (iv) development of UHR LVSEM, by which uncoated biological specimens can be observed under LV and (v) establishment of the ULT/LVSEM method.

The studies by means of EM will continue as important and powerful techniques for obtaining extensive information on biological structure in the 21st century, since the study of 3D will become subjective. The identification of the gene expression and proteins will become possible by the established cryo-technique, especially freeze replica combined with SDS-FRL and STEM of the same specimen. The juncture of CEMOVIS [110] with IEM will be the key to the resolution of research in cell biology. Furthermore, the integration of live cell imaging and super resolution fluorescence microscopy, which has been developed by a new theory, will be aniticipated as a new method for resolving the movement of functional molecules in cells the near future.

In the past, we constructed 3D images by successive serial sectioning of the biological specimen [65,74]. In contrast, the methods for reconstructing 3D images by FIB SEM [111] or SBF SEM are powerful and quick techniques. Recently, we have been able automatically to obtain 600 serial images from a whole *S. pombe* cells for only 20 h by FIB SEM [112]. This makes us able to analyze the 3D architecture of the cell.

Thus the techniques for observing and analyzing ultrastructures of molecules as well as intracellular organelles have developed significantly, and now it is possible to obtain image information with high quality. However, to understand the meaning of

observations, it is necessary to accumulate basic knowledge of morphology rather than to rely upon the technique.

Supplementary data

Supplementary data are available at http://jmicro.oxfordjournals.org/.

Funding

The work was supported by grant-in-aid for scientific research from the Ministry of Education, Culture, Sport, Science and Technology of Japan (No. 11640668, 13640670, 15570053) and the Open Research Center (013019, 010013) and the Bio-imaging Center (S0991025) of JWU established in private universities in Japan with the support of the Ministry of Education, Culture, Sports Science and Technology.

Acknowledgements

My works hitherto are largely due to the kind leadership of the following scholars: the late Professor S. Fukui, Professor A. Tanaka and M. Ueda of the Kyoto University for the research of microbody, Professor M. Yanagida of the Kyoto University for the optical diffraction and filtering, Professor N. Baba of Kogakuin University for image reconstruction and analysis, and Professor H. Ohno of Tokyo Phar. University for the analysis of the cell wall of *S. pombe*. I would like to express my sincere thanks to them. I also express my great thanks to JEOL Ltd., Hitachi High-Technologies Corporation, FEI Company and Ratoc System Engineering Co Ltd. for the use of the companies' most modern EM equipment. My large gratitude is also due to Ms N. Yamada, Dr M. Sato, Dr S. Isijima, Ms Y. Kondo, Ms Y. Tsukamoto, N. Moritoki, A. Takahashi and S. Matumoto of the Electron Microscopic Laboratory of the Japan Women's University, and Professor H. Kobori, Dr M. Baba, Dr N. Kamasawa, Ms H. Kokuba, Dr M. Konomi, Dr T. Takagi, Dr T. Kamasaki, Ms Y. Sibasaki, Ms T. Sugahwara, Ms Y. Ikeda and Ms K. Ajima, Ms E. Tao of Professor Osumi Laboratory in the graduate school of Japan Women's University for their useful help in my research. Finally I must express my sincere thanks to Professor M. Sameshima of Hirosaki University, for his large endeavor to examine my draft of the present paper thoroughly.

References

1 Agar H D and Douglas H C (1957) Studies on the cytological structure of yeast: electron microscopy of thin sections. *J. Bacteriol.* **73**: 365–375.

2 Matile P, Moor H, and Robinow C F (1969) Yeast cytology. In: Rose A H and Harrison J S (eds.), *The Yeasts*, pp 219–302 (Academic Press, New York).

3 Osumi M (1965) Electron-microscopical observations on the formation of yeast-mitochondria. Bot. Mag. *(Tokyo)* **78**: 231–239.

4 Osumi M and Sando N (1969) Division of yeast mitochondria in synchronous culture. *J. Electron Microsc.* **18**: 47–56.

5 Kitamura K, Kaneko T, and Yamamoto Y (1971) Lysis of viable yeast cells by enzymes of *Arthrobacter luteus*. *Arch. Biochem. Biophys.* **145**: 402–405.

6 Osumi M, Imaizumi F, Imai M, Sato H, and Yamaguchi H (1975a) Isolation and characterization of microbodies from *Candida tropicalis* pk233 cells grown on normal alkanes. *J. Gen. Appl. Microbiol.* **21**: 375–387.

7 Baba M and Osumi M (1987) Transmission and scanning electron microscopic examination of intracellular organelles in freeze-substituted *Kloeckera* and *Saccharomyces cerevisiae* yeast cells. *J. Electron Microsc. Tech.* **5**: 249–261.

8 Osumi M, Baba M, Naito N, Taki A, Yamada N, and Nagatani T (1988) High resolution low voltage scanning electron microscopy of uncoated yeast cells fixed by the freeze-substitution method. *J. Electron Microsc.* **37**: 17–30.

9 Osumi M (1998a) The ultrastructure of yeast: cell wall structure and formation. *Micron* **29**: 207–233.

10 Murai T, Ueda M, Yamamura M, Atomi H, Shibasaki Y, Kamasawa N, Osumi M, Amachi T, and Tanaka A (1997a) Construction of a starch-utilizing yeast by cell surface engineering. *Appl. Environ. Microbiol.* **63**: 1362–1366.

11 Murai T, Ueda M, Atomi H, Shibasaki Y, Kamasawa N, Osumi M, Kawaguchi T, Arai M, and Tanaka A (1997b) Genetic immobilization of cellulase on the cell surface of *Saccharomyces cerevisiae*. *Appl. Microbiol. Biotechnol.* **48**: 499–503.

12 Kamasawa N, Yoshida T, Ueda M, Tanaka A, and Osumi M (1999) Three-dimensional analysis of protein aggregate body in *Saccharomyces cerevisiae* cells. *J. Electron Microsc.* **48**: 173–176.

13 Humbel B M, Konomi M, Takagi T, Kamasawa N, Ishijima S A, and Osumi M (2001) *In situ* localization of beta-glucans in the cell wall of *Schizosaccharomyces pombe*. *Yeast* **18**: 433–444.

14 Konomi M, Fujimoto K, Toda T, and Osumi M (2003) Characterization and behavior of α-glucan synthase in *Schizosaccharomyces pombe* as revealed by electron microscopy. *Yeast* **20**: 427–438.

15 Osumi M, Shimoda C, and Yanagishima N (1974) Mating reaction in *Saccharomyces cerevisiae* .V. Changes in the fine structure during the mating reaction. *Arch. Microbiol.* **97**: 27–38.

16 Ludvík J, Munk V, and Dostálek M (1968) Ultrastructural changes in the yeast *Candida lipolytica* caused by penetration of hydrocarbons into the cell. *Experientia* **24**: 1066–1068.

17 Messel M N, Medvedeva G A, Kozlova T M, Pomoshnikova N A, Zaikina A I, and Fedoseeva G E (1973) Regularities of penetration into yeast cells of higher fatty acids and hydrocarbons, their intracellular migration and concentration. In: Proc. 3rd Internatl. Symp. Yeasts, pp 149–168 (Otaniemi, Helsinki, Finland).

18 Fukui S and Osumi M (1973) Some specific features of the ultrastructure of Candida yeast cells growing on hydrocarbons. In: Proc. 3rd Symp. Technical Microbiol., pp 375–384 (Berlin).

19 Hruban Z and Rechcigl M, Jr (1969) *Microbodies and Related Particles (Morphology, Biochemistry, and Physiology)*, (Academic Press, New York).

20 Tolbert N E (1971) Microbodies-peroxisomes and glyoxysomes. *Ann. Rev. Plant Physiol.* **22**: 45–74.

21 Osumi M, Miwa N, Teranishi Y, Tanaka A, and Fukui S (1974) Ultrastructure of *Candida* yeasts grown on *n*-alkanes: appearance of microbodies and its relationship to high catalase activity. *Arch. Microbiol.* **99**: 181–201.

22 Osumi M, Fukuzumi F, Teranishi Y, Tanaka A, and Fukui S (1975) Development of microbodies in *Candida tropicalis* during incubation in a *n*-alkane medium. *Arch. Microbiol.* **103**: 1–11.

23 Teranishi Y, Tanaka A, Osumi M, and Fukui S (1974) Catalase activities of hydrocarbon-utilizing *Candida yeasts*. *Agr. Biol. Chem.* **38**: 1213–1220.

24 Teranishi Y, Kawamoto S, Tanaka A, Osumi M, and Fukui S (1974) Induction of catalase activity by hydrocarbons in *Candida tropicalis* pK 233. *Agr. Biol. Chem.* **38**: 1221–1225.

25 Kawasaki N, Ikeda Y, Kamasawa N, Aoyam K, and Osumi M. Zipper-like structure in yeast peroxisome. (in preparation).

26 Fujiwara T, Kuroiwa H, Yagisawa F, Ohnuma M, Yoshida Y, Yoshida M, Nishida K, Misumi O, Watanabe S, Tanaka K, and Kuroiwa T (2010) The coiled-coil protein VIG1 is essential for tethering vacuoles to mitochondria during vacuole inheritance of *Cynanidioschyz*on *merolae*. *Plant Cell* **22**: 772–781.

27 Escaño C S, Juvvadi P R, Jin F J, Takahashi T, Koyama Y, Yamashita S, Maruyama J, and Kitamoto K (2009) Disruption of the A*opex11–1* gene involved in peroxisome proliferation leads to impaired Woronin body formation in *Aspergillus oryzae*. *Eukaryot. Cell* **8**: 296–305.

28 de Duve C (1973) Biochemical studies on the occurrence, biogenesis and life history of mammalian peroxisomes. *J. Histochem. Cytochem.* **21**: 941–948.

29 Kamasawa N (2001) Ultrastructural Studies of Biogenesis of Yeast Peroxisome. Doctor Thesis of Japan Women's University, pp 85 (in Japanese).

30 Kamasawa N and Osumi M (2001) Biogenesis of yeast peroxisomes. *J. Electron Microsc.* **36**: 138–140. (in Japanese).

31 Miyagishima S, Itoh R, Toda K, Kuroiwa H, Nishimura M, and Kuroiwa T (1999) Microbody proliferation and segregation cycle in the single-microbody alga *Cyanidioschyzon merolae*. *Planta* **208**: 326–336.

32 van der Zand A, Gent J, Braakman I, and Tabak H F (2012) Biochemically distinct vesicles from the endoplasmic reticulum fuse to form peroxisomes. *Cell* **149**: 397–409.

33 Hoepfner D, Schildknegt D, Braakman I, Philippsen P, and Tabak H F (2005) Contribution of the endoplasmic reticulum to peroxisome formation. *Cell* **122**: 85–95.

34 Nuttall J M, Motley A, and Hettema E H (2011) Peroxisome biogenesis: recent advances. *Curr. Opin. Cell Biol.* **23**: 421–426.

35 Kamasawa N, Naito N, Kurihara T, Kamada Y, Ueda M, Tanaka A, and Osumi M (1992) Immunoelectron microscopic localization of thiolases, beta-oxidation enzymes of an *n*-alkane-utilizable yeast, *Candida tropicalis*. *Cell Struct. Funct.* **17**: 203–207.

36 Kamasawa N, Ohtsuka I, Kamada Y, Ueda M, Tanaka A, and Osumi M (1996) Immunoelectron microscopic observation of the behaviors of peroxisomal enzymes inducibly synthesized in an *n*-alkane-utilizable yeast cell, *Candida tropicalis*. *Cell Struct. Funct.* **21**: 117–122.

37 Kamasawa N, Yoshida T, Kasahara M, Kamada Y, Zou W, Ueda M, Tanaka A, and Osumi M (1996) Subcellular destination of mutant peroxisomal isocitrate lyase polypeptides of *Candida tropicalis* in *Saccharomyces cerevisiae*. *J. Electron Microsc.* **45**: 491–497.

38 Fukui S, Tanaka A, Kawamoto S, Yasuhara S, Teranishi Y, and Osumi M (1975) Ultrastructure of methanol-utilizing yeast cells: appearance of microbodies in relation to high catalase activity. *J. Bacteriol.* **123**: 317–328.

39 Tanaka A, Yasuhara S, Kawamoto S, Fukui S, and Osumi M (1976) Development of microbodies in the yeast *Kloechera* growing on methanol. *J. Bacteriol.* **126**: 919–927.

40 Osumi M and Sato M (1978) Further studies on the localization of catalase in yeast microbodies by ultrathin frozen sectioning. *J. Electron Microsc.* **27**: 127–136.

41 Osumi M, Sato M, Sakai T, and Suzuki M (1979) Fine structure of crystalloid in the yeast *Kloeckera* microbodies. *J. Electron Microsc.* **28**: 295–300.

42 Hosoi J and Osumi M (1981) Alternate arrangement of large and small particles in crystalloid of *Kloeckera* yeast microbody of halite structure type. *J. Electron Microsc.* **30**: 158–160.

43 Hosoi J and Osumi M (1981) Confirmation of composite crystal model of the crystalloid of *Kloeckera* microbody by optical transforms. *J. Electron Microsc.* **30**: 321–326.

44 Osumi M, Sato M, and Nagano M (1981) Structure of the microbody crystalloid in methanol grown yeast as a composite crystal of catalase and alcohol oxidase. In: Stewart G G and Russell I (eds.), *Current Developments in Yeast Research*, pp 69–74 (Pergamon Press, Canada).

45 Osumi M, Nagano M, Yamada N, Hosoi J, and Yanagida M (1982) Three-dimensional structure of the crystalloid in the microbody of *Kloeckera* sp.: composite crystal model. *J. Bacteriol.* **151**: 376–383.

46 Kanaya K, Baba N, Shinohara C, and Osumi M (1983) A digital processing method for the structural analysis of lattice images of crystalloids obtained by electron microscopy. *Micron Microsc. Acta* **14**: 233–247.

47 Baba N, Nagano M, Osumi M, and Kanaya K (1984) A study on the unit cell structure of the crystalloid in the *Kloeckera* microbody using digital image processings and computer simulations. *J. Electron Microsc.* **33**: 203–216.

48 De Rosier D J and Klug A (1972) Structure of the tubular variants of the head of bacteriophage T4 (polyheads). *J. Mol. Biol.* **65**: 469–488.

49 Sando N (1963) Biochemical studies on the synchronized culture of *Schizosaccharomyces pombe*. *J. Gen. Appl. Microbiol.* **9**: 233–241.

50 Mitchison J M, Cummins J E, Gross P R, and Creanor J (1969) The uptake of bases and their incorporation into RNA during the cell cycle of *Schizosaccharomyces pombe* in normal growth and after a step-down. *Exp. Cell Res.* **57**: 411–422.

51 Marks J and Hyams J S (1985) Localization of F-actin through the cell division cycle of *Schizosaccharomyces pombe*. *Eur. J. Cell Biol.* **39**: 27–32.

52 Marks J, Hagan I M, and Hyams J S (1986) Growth polarity and cytokinesis in fission yeast: the role of the cytoskeleton. *J. Cell Sci. Suppl.* **5**: 229–241.

53 Hagan I and Hyams J (1988) The use of cell division cycle mutants to investigate the control of microtubule distribution in the fission yeast *Schizosaccharomyces pombe*. *J. Cell Sci.* **89**: 343–357.

54 Hagan I and Yanagida M (1997) Evidence for cell cycle-specific, spindle pole body-mediated, nuclear positioning in the fission yeast *Schizosaccharomyces pombe*. *J. Cell Sci.* **110**: 1851–1866.

55 Su S S Y and Yanagida M (1997) Mitosis and cytokinesis in the fission yeast, *Schizosaccharomyces pombe*. The yeast cytoskeleton. In: Pringle J P, Broach J B, and Jones E W (eds.), *The Molecular and Cellular Biology of the Yeast Saccharomyces III*, pp 765–826 (Cold Spring Harbor Laboratory Press, New York).

56 Tatebe H, Goshima G, Takeda K, Nakagawa T, Kinoshita K, and Yanagida M (2002) Fission east living mitosis visualized by GFP-tagged gene products. *Micron* **32**: 67–74.

57 Arai R and Mabuchi I (2002) F-actin ring formation and the role of F-actin cables in the fission yeast *Schizosaccharomyces pombe*. *J. Cell Sci.* **115**: 887–898.

58 Verde F (1998) On growth and form: control of cell morphogenesis in fission yeast. *Curr. Opin. Microbiol.* **1**: 712–718.

59 Kobori H, Yamada N, Taki A, and Osumi M (1989) Actin is associated with the formation of the cell wall in reverting protoplasts of the fission yeast *Schizosaccharomyces pombe*. *J. Cell Sci.* **94**: 635–646.

60 Hoch H C and Howard R J (1980) Ultrastructure of freeze-substituted hyphae of the basidiomycete *Laetisaria arvalis*. *Protoplasma* **103**: 281–297.

61 Naito N, Yamada N, Kobori H, and Osumi M (1991) Contrast enhancement by ruthenium tetroxide for observation of the ultrastructure of yeast cells. *J. Electron Microsc.* **40**: 416–419.

62 Kamasaki T, Arai R, Osumi M, and Mabuchi I (2005) Directionality of F-actin cables changes during the fission yeast cell cycle. *Nature Cell Biol.* **7**: 916–917.

63 Kamasaki T, Osumi M, and Mabuchi I (2007) Three-dimensional arrangement of F-actin in the contractile ring of fission yeast. *J. Cell. Biol.* **178**: 765–771.

64 Takagi T (2003) Ultrastructure Analysis of the Actin Cytoskeleton in Fission Yeast. Doctor Thesis of Japan Women's University, pp 102 (in Japanese).

65 Takagi T, Ishijima S A, Ochi H, and Osumi M (2003) Ultrastructure and behavior of actin cytoskeleton during cell wall formation in the fission yeast *Schizosaccharomyces pombe*. *J. Electron Microsc.* **52**: 161–174.

66 Osumi M (2002) On the ultrastructure of yeast cells. *Plant Morphol.* **14**: 54–67. (in Japanese)

67 Osumi M (2002) The significance of high pressure freezing technique in structural biology. With reference to a study of cell wall formation in fission yeast. J. Japan Woman's Univ. Faculty of Science. **10**: 43–63. (in Japanese).

68 Osumi M, Konomi M, Sugawara T, Takagi T, and Baba M (2006) High-pressure freezing is a powerful tool for visualization of *Schizosaccharomyces pombe* cells: ultra-low temperature and low-voltage scanning electron microscopy and immunoelectron microscopy. *J. Electron Microsc.* **55**: 75–88.

69 Konomi M (2005) Ultrastructural studies on cell wall and septum formation in fission yeast. *Plant Morphol.* **17**: 35–44 (in Japanese).

70 Sato M, Otsuka S, Miyamoto R, and Osumi M (1989) Development of low-voltage and high resolution SEM. I. Instrumentation. *Biomed. SEM* **18**: 1–3. (in Japanese).

71 Nagatani T, Sato M, and Osumi M (1990) Development of an ultra-high-resolution low voltage (LV) SEM with an optimized 'in-lens' design. In: Proc. 12th Int. Congr. Electron Microsc., pp 388–389 (Seattle).

72 Osumi M, Yamada N, Yaguchi H, Kobori H, Nagatani T, and Sato M (1995) Ultrahigh-resolution low-voltage SEM reveals ultrastructure of the glucan network formation fission yeast protoplast. *J. Electron Microsc.* **44**: 198–206.

73 Osumi M (2011) Coating method for ultra-high vacuum and ultra-low temperature. In: Kanto Branch of Jap. Soci. Microscopy (ed.), *SHIN-SOSA DENSHI KENBIKYO*, pp 182 (Kyoritsu-Shuppan Co. Ltd., Tokyo). (in Japanese).

74 Osumi M, Sato M, Ishijima S A, Konomi M, Takagi T, and Yaguchi H (1998c) Dynamics of cell wall formation in fission yeast, *Schizosaccharomyces pombe*. *Fungal Genet. Biol.* **24**: 178–206.

75 Osumi M, Yamada N, Kobori H, Taki A, Naito N, Baba M, and Nagatani T (1989b) Cell wall formation in regenerating protoplast of *Schizosaccharomyces pombe:* study by high-resolution low-voltage scanning electron microscopy. *J. Electron Microsc.* **38**: 457–468.

76 Osumi M, Baba M, and Yamaguchi H (1984) Electron microscopical study on the biosynthesis and assembly of yeast cell wall components. In: Nombela C (ed.), *Cell Wall Synthesis and Autolysis*, pp 137–142 (Elsevier Science, Amsterdam).

77 Yamaguchi H, Hiratani T, Baba M, and Osumi M (1985) Effect of aculeacin A, a wall-active antibiotic, on synthesis of the yeast cell wall. *Microbiol. Immunol.* **29**: 609–623.

78 Yamaguchi H, Hiratani T, Baba M, and Osumi M (1987) Effect of aculeacin A on reverting protoplasts of *Candida albicans*. *Microbiol. Immunol.* **31**: 625–638.

79 Osumi M, Yamada N, Kobori H, and Yamaguchi H (1992) Observation of colloidal gold particles on the surface of yeast protoplasts with UHR-LVSEM. *J. Electron Microsc.* **41**: 392–396.

80 Sugawara T, Takahashi S, Osumi M, and Ohno N (2004) Refinement of the structure of cell wall glucans of *Shizosaccharomyces pombe* by chemical modification and NMR spectroscopy. *Carbohydr. Res.* **339**: 2255–2265.

81 Sugawara T, Sato M, Takagi T, Kamasaki T, Ohno N, and Osumi M (2003) *In situ* localization of cell wall α-1,3-glucan in the fission yeast *Schizosaccharomyces pombe*. *J. Electron Microsc.* **52**: 237–242.

82 Sugawara T, Takagi T, Sato M, Ohno N, and Osumi M (2001) Architecture and localization of the cell wall glucans of the fission yeast, *Schizosaccharomyces pombe*. In: Proc. Mol. Mechanisms of Fungal Cell Wall Biogenesis, pp 61 (Ascona, Switzerland).

83 Manners D J, Masson A J, and Patterson J C (1973) The structure of a β-(1, 3)-D-glucan from yeast cell walls. *Biochem. J.* **135**: 19–30.

84 Ranvier L (1887) De l'emploi de l'acide perruthenique dans les recherchés histologiques, et de l'application de ce réactif à l'étude des vacuoles des cellules caliciformes. *C R Hebd. Seances Acad. Sci.* **105**: 145.

85 Carpenter D C and Nebel B R (1931) Ruthenium tetroxide as a fixative in cytology. *Science* **74**: 154–155.

86 Bahr G F (1954) Osmium tetroxide and ruthenium tetroxide and their reactions with biologically important substances. *Exp. Cell Res.* **7**: 457–479.

87 Ishiguro J and Kobayashi W (1996) An actin point-mutation neighboring the 'hydrophobic plug' causes defects in the maintenance of cell polarity and septum organization in the fission yeast *Schizosaccharomyces pombe*. *FEBS Lett.* **392**: 237–241.

88 Ishijima S A, Konomi M, Takagi T, Sato M, Ishiguro J, and Osumi M (1999) Ultrastructure of cell wall of the *cps8* actin mutant cell in *Schizosaccharomyces pombe*. *FEMS Microbiol. Lett.* **180**: 31–37.

89 Konomi M, Ishiguro J, and Osumi M (2000) Abnormal formation of the glucan network from regenerating protoplasts in *Schizosaccharomyces pombe cps8* actin point mutant. *J. Electron Microsc.* **49**: 569–578.

90 Kitayama S, Hirata D, Arellano M, Pérez P, and Toda T (1999) Fission yeast α-glucan synthase mok1 requires the actin cytoskeleton to localize the site of growth and plays an essential role in cell morphogenesis downstream of protein kinase C function. *J. Cell Biol.* **144**: 1173–1186.

91 Klis F M (1994) Review: cell wall assembly in yeast. *Yeast* **10**: 851–869.

92 Klis F M, Boorsma A, and Groot P W (2006) Cell wall construction in *Saccharomyces cerevisiae*. *Yeast* **23**: 185–202.

93 de Nobel H and Lipke P N (1994) Is there a role for GPIs in yeast cell-wall assembly? *Trends Cell Biol.* **4**: 42–45.

94 Lipke P N and Ovalle R (1998) Cell wall architecture in yeast: new structure and new challenges. *J. Bacteriol.* **180**: 3735–3740.

95 Kapteyn J C, Montijn R C, Vink E, de la Cruz J, Llobell A, Douwes J E, Shimoi H, Lipke P N, and Klis F M (1996) Retention of *Saccharomyces cerevisiae* cell wall proteins through a phosphodiester-linked β-1,3-/β-1,6-glucan heteropolymer. *Glycobiology* **6**: 337–345.

96 Schreuder M P, Brekelmans S, Van den Ende H, and Klis F M (1993) Targeting of a heterologous protein to the cell wall of *Saccharomyces cerevisiae*. *Yeast* **9**: 399–409.

97 Aimanianda V, Clavaud C, Simenel C, Fontaine T, and Delepierre M (2009) Cell wall β-(1,6)-glucan of *Saccharomyces cerevisiae*. Structural characterization and *in situ* synthesis. *J. Biol. Chem.* **15**: 13401–13412.

98 Osumi M (2009) Research into yeasts focusing on its cell wall formation. *J. SJWS.* **10**: 17–40. (in Japanese)

99 Sluder D and Muller M M (1989) High pressure freezing comes of age. *Scanning Microsc. Suppl.* **3**: 253–269.

100 Fujimoto K (1995) Freeze-fracture replica electron microscopy combined with SDS digestion for cytochemical labeling of internal membrane proteins. Application to the immunogold labeling of intercellular junctional complexes. *J. Cell Sci.* **108**: 3443–3449.

101 Cortes J C G, Sato M, Munoz J, Moreno M B, Clemente-Ramos J A, Romas M, Okada H, Osumi M, Duran A, and Ribas J C (2012)

Fission yeast Ags1 confers the essential septum strength needed for safe gradual cell abscission. *J. Cell Biol.* **198**: 637–656.

102 Kamino T, Yaguchi T, Ohnishi T, Ishitani T, and Osumi M (2004) Application of a FIB-STEM for 3D observation of a resin-embedded yeast cell. *J. Electron Microsc.* **53**: 563–566.

103 Osumi M, Kamino T, Yaguchi T, Sano T, Ohnishi T, and Ishitani T (2006) A new application of the FIB-STEM system for the 3D observation of yeast cells. In: Proc. 16th Int. Microsc. Congress, pp 435 (Sapporo).

104 Kamino T, Yaguchi N, Sato T, and Onishi T (2006) Application of FIB technique to 3D observation of resin embedded biological tissues. In: Proc. Microsc. Microanal., pp 1232–1233 (Chicago).

105 Osumi M, Eguchi T, Yaguchi T, Sato T, and Okada H (2010) Tree dimensional obserbation of yeast cells and baculovirus pioneered by FIB-micro sampling. *J. Bacteriol.* **65**: 225.

106 Yaguchi N, Sto T, Eguchi T, Okada H, and Osumi M (2010) Visualization of specific yeast cell wall by FIB-STEM. *J. Bacteriol.* **65**: 108.

107 Aoyama K, Takagi T, Inoke K, Mabuchi I, and Osumi M (2006) Multi section electron tomography. In: Proc. 16th Int. Microsc. Congress, pp 710 (Sapporo).

108 Aoyama K, Takagi T, Hirase A, and Miyazawa A (2008) STEM tomography for thick biological specimens. *Ultramicroscopy* **109**: 70–80.

109 Aoyama K, Takagi T, Noda T, and Morone N (2008) Electron tomography for thick biological specimens by using scanning transmission technique. In: Proc. 9th Asia Pacific Microsc. Conf., pp 960–961 (Chejudo).

110 Pierson J, Vos M, McIntosh J R, and Peters P J (2011) Perspectives on electron cryo-tomography of vitreous cryo-sections. *J. Electron Microsc.* **60**: S93–S100.

111 Wei D, Jacobs S, Modla S, Zhang S, Young C L, Cirino R, Caplan J, and Czymmek K (2012) High-resolution three-dimensional reconstruction of a whole yeast cell using focused-ion beam scanning electron microscopy. *Biotechniques* **53**: 41–48.

112 Osumi M, Nakano K, and Okada H. Three-demensional reconstruction of synchronous culturerd *S. pombe* cells using FIB-SEM. (in preparation).